Electrical Breakdown of Thermal Spray Alumina Ceramic Applied to AlSiC Baseplates Used in Power Module Packaging

by

Charles W. Mossor

Thesis submitted to the Faculty of the

Virginia Polytechnic Institute and State University

in partial fulfillment of the requirements for the degree of

Master of Science

In

Electrical Engineering

Dr. A. Elshabini, Chairman

Dr. P. Athanas

Dr. W. Baumann

June 11, 1999

Blacksburg, Virginia

Keywords: Thermal Spray, Dielectric Strength, Breakdown Voltage, Metal Matrix Composite, and Power Packaging.

Electrical Breakdown of Thermal Spray Alumina Ceramic Applied to AlSiC Baseplates Used in Power Module Packaging

by

Charles W. Mossor
Committee Chairman: A. Elshabini
The Bradley Department of Electrical & Computer Engineering

EXECUTIVE SUMMARY

Thermal spray coatings offer new alternatives in the production of electronic power modules that use alumina ceramic as an isolation layer. Current processes use direct bond copper (DBC) soldered to a nickel plated copper heat spreader. A coefficient of thermal expansion (CTE) mismatch exists between copper and alumina and leads to reliability issues that arise due to product failure during thermal cycling and lifetime operation. The substitution of an AlSiC metal matrix composite (MMC) heat spreader baseplate addresses the problem of CTE mismatch and will reduce the number of product failures related to cracking and delamination caused by this pronounced mismatch in the thermal expansion coefficient..

The substitution of an AlSiC (MMC) heat spreader baseplate also allows the production process to be achieved with a fewer number of metallization layers. Thermal spray can apply alumina ceramic coatings directly to the AlSiC (MMC) baseplates. A reduction in process steps will lead to a reduction in manufacturing costs, the main driving objective in Microelectronics Industries.

Thermal spray coatings have a major problem since they have a porous microstructure which can trap undesired moisture. The moisture basically causes the

coatings to have a lower dielectric breakdown voltage and a higher leakage current at normal operating voltages. This problem can be eliminated by manufacturing the electronic power modules in a controlled environment and packaging the devices in a hermetically sealed package.

This thesis analyzes the data obtained from direct-voltage dielectric breakdown and direct-voltage leakage current tests conducted on coupons manufactured using the thermal plasma spray coating process and the thermal high-velocity oxyfuel (HVOF) coating process. ASTM specifications defining appropriate testing procedures are used in testing the dielectric strength of these coupons.

Issues relating to the dielectric strength and dielectric leakage current are evaluated and validated at the Microelectronics Laboratory at Virginia Polytechnic Institute & State University. The objective to conduct this research study using plasma and HVOF alumina coatings as dielectric isolation layers is to support the Microelectronics Industries in developing a product with increased reliability at a lower manufacturing cost.

Acknowledgments

I would like to thank my advisor, Dr. Elshabini, for her continued dedication and support of my research. Her guidance has led me to a bright and exciting career. I would also like to thank my other Committee members, Dr. P. Athanas, and Dr. W. Baumann for taking the time to serve on my committee.

I would like to thank my mother and Major for supporting me in my endeavors all these years. I would like to thank my wife and son for the patience put forward while I pursued my ambitions. I would like to thank my father for setting the example. It was his belief that I could accomplish anything I set my mind to.

I would like to thank Fred, Rich, Alex, James and Suwanna for their assistance in my work. I would like to thank Mike Oberle for assisting with Labview™. The Microelectronics Laboratory was an adventurous place in which to work and study. I would like to thank Paul for being a friend and for the competition between friends.

I appreciate greatly the financial support of Lanxide Electronic Components.

Thank you all for your help and dedication.

TABLE OF CONTENTS

LIST OF FIGURES

LIST OF TABLES

CHAPTER 1

INTRODUCTION

1.1 Identification of Problem

This thesis is concerned with the topic of electronic power module packaging and the components that make up electronic power modules used for electric motor drives and electric vehicles. Today's high power modules normally consist of direct bond copper (DBC) on ceramic soldered to a copper base plate.[1] Electronic devices such as IGBTs are soldered to the DBC layer and wirebonded to achieve the final electrical connections. Heavy-duty metal pins or clips provide the I/O connections and allow for direct attachment to high power busbars. The electronic components are encapsulated in silicon and the electronic power module is packaged in a plastic housing.

The objective is to make the modules smaller in size while enabling them the capability to withstand a larger supply of power. Thermal management becomes a major concern as more heat is generated within a smaller boundary. The use of copper baseplates provides a large heat spreader to dissipate the heat away from the power component. On the other hand, the use of these materials cause a secondary problem in the form of coefficient of expansion (CTE) mismatch, affecting the reliability of these products over lifetime operation under load manifested with thermal cycling testing.

CTE mismatch arises when two materials, possessing different rates of thermal expansion, are soldered together. As the component goes through thermal cycling or normal operating conditions, one material expands or contracts at a faster rate than the

other material. This effect creates a tearing stress at the interface and leads to fractures, delaminated layers/films, and component failure. Copper (Cu) has a CTE of 17 ppm/ºK while the alumina (Al_2O_3) ceramic has a CTE of 6-7 ppm/ºK. The large difference of CTE between Cu and alumina causes many reliability problems in electronic power modules. The alumina provides electrical isolation between the grounded baseplate and the power devices. If a fracture develops within the alumina due to thermal cycling, a short would occur and the module would likely fail.

One alternative is to use a metal-matrix composite (MMC) to replace the copper.[1] MMC is composed of a ceramic or graphite matrix injected with a metal such as Aluminum (Al). Aluminum-Silicon-Carbide (AlSiC) is a MMC replacement candidate for Cu baseplates since its CTE is 7-8 ppm/ºK, which is a closer match to alumina's CTE. Matching the CTE's prevents delamination and cracking occurence at the interface, thus leading to a more reliable product. The tradeoff of matching the CTEs of materials is a reduction in thermal capacity. The thermal conductivity of Cu is 393 W/mºK, while the thermal conductivity of AlSiC is of the order 175-218 W/mºK. The ability to remove the proper heat during operation becomes a critical factor to consider. If the operating temperature becomes too high, the component will burn out and failure will result. Proper analysis of the maximum operating temperature will determine whether the Cu baseplate can be replaced by a MMC baseplate.

1.2 Nature of Work, Objectives, and Goals

This research studies the electrical isolation provided by thermal spray alumina applied to AlSiC MMC baseplates. Two different techniques of thermal spray systems are evaluated in this work; Plasma Spray and High-Velocity Oxyfuel (HVOF). In a plasma spray system, both the heat source and the propelling agent are provided by the plasma forming gas.[2] A high voltage arc excites a plasma forming gas which is then forced through a convergent/divergent nozzle to form a high velocity plasma flame. Upon introduction of alumina powder into the flame, the alumina melts into tiny particles and is bombarded onto the target surface where it cools into a dielectric coating.

HVOF thermal spray coatings are produced when oxygen and fuel are mixed in a chamber and the products of combustion exit through a nozzle at a supersonic speed.[3] Alumina powder is introduced in the nozzle, melted, and expelled with the gases toward the target. Particle velocities can reach speeds of the order 550 m/s.

Electrical isolation is checked by breakdown voltage tests conducted on coupons of AlSiC MMC baseplates with thermal spray alumina applied as the insulator. Leakage current and electrical breakdown are measured through the bulk alumina as well as leakage current across the surface of the alumina. The goal is to insure electrical isolation between the power devices and the AlSiC MMC baseplates.

1.3 Techniques Used

A 20 KV power supply controlled by a Labview™ program is used to measure the electrical breakdown voltage and leakage currents. The baseplates are mounted in a grounded metal case with a positive voltage pin coming in contact with the alumina ceramic. The voltage of the power supply is stepped up until the device under test (DUT) fails. The same apparatus is used to measure the bulk leakage current, but the voltage is not driven high enough to cause electrical breakdown.

A similar apparatus is used to check the leakage current with the addition of a resistive network and a digital multimeter used to amplify the resolution of the leakage current. The leakage current is tested at normal working voltages and is a non-distructive test.

1.4 Technical Achievements and Contributions

The work and research presented in the thesis is intended to demonstrate the electrical isolation provided by thermal spray alumina ceramic applied to AlSiC MMC baseplates. Experiments will show the importance of preventing moisture from being absorbed by the porous thermal spray alumina ceramic. The absorption of moisture will reduce the dielectric breakdown significantly. Characterization to leakage currents provides information concerning the quality of thermal spray alumina ceramic used to provide electrical isolation in electronic power module baseplates. The findings of this

research work are beneficial as industry examines alternatives of using AlSiC MMC baseplates to replace or substitute copper baseplates.

1.5 Structure of Thesis

This thesis is presented in six Chapters. The First chapter is the general Introduction. Chapter Two discusses electronic power module baseplates and the reliability issues encountered with their production and applications. Problems associated with using copper baseplates are presented along with alternatives for corrective solutions. Chapter Three is a review of the thermal spray processes. Applying alumina to AlSiC MMC baseplates using HVOF and plasma spray processes are examined. Application techniques and microstructure physics are also reviewed in this Chapter. Chapter Four is concerned with electrical breakdown techniques. Testing procedures for measuring electrical breakdown voltage and leakage currents are used to construct the necessary testing fixtures employed during the thesis research. Chapter Five presents the results obtained through experiments conducted in the Microelectronics Laboratory at Virginia Polytechnic Institute and State University on the electrical isolation characteristics of thermal spray alumina. Finally, Chapter Six summarizes the work conducted in this thesis, and presents recommendations for future work pertaining to the area of thermal spray alumina applied to AlSiC MMC baseplates and the electrical isolation they provide.

CHAPTER 2

POWER MODULE BASEPLATES

2.1 Introduction

Electronic power modules are used throughout the consumer and commercial marketplace. Industry uses high power modules to deliver high current and/or high voltage to electric vehicles, electric power supplies, and electric motor drives. The enormous amount of heat dissipated by a power module leads to a reliability concern since the module will burn up if the heat is not properly managed. Thermal cycling also presents a reliability issue since the heating and cooling ties to the expansion and contraction of the composite materials which leads to cracking, delamination, and eventual failure.

2.2 Background and Concept

Today's high power modules normally consist of direct bond copper (DBC) on ceramic soldered to a copper base plate. Electronic devices such as IGBTs are soldered to the DBC layer and wirebonded to achieve the final electrical connections. Figure 2.1 shows the configuration of the metallization and insulative layers. Heavy-duty metal pins or clips provide the I/O connections and allow for direct attachment to high power bussbars. The electronic components are encapsulated in silicon and the electronic power module is packaged in a plastic housing.

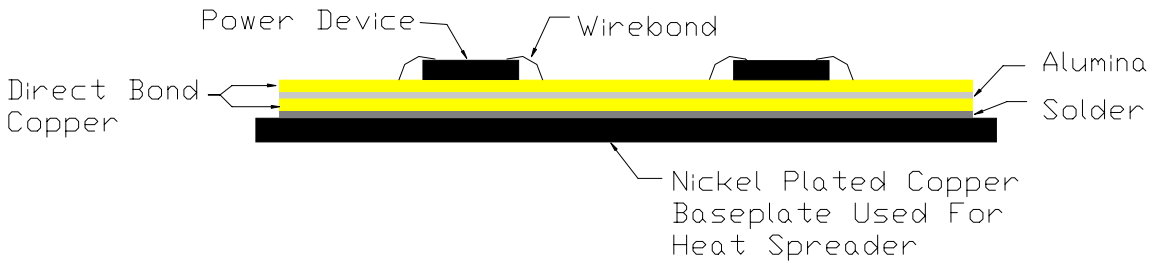

Figure 2.1. Electronic Power Module Using Direct Bond Copper.

The objective is to make the modules smaller in size while enabling them the capability to withstand a larger supply of power. Thermal management becomes a major concern as more heat is generated within a smaller boundary. The use of copper baseplates provides a large heat spreader to dissipate the heat away from the power component. On the other hand, the use of these materials cause a secondary problem concerning the coefficient of thermal expansion (CTE) mismatch.

CTE mismatch arises when two materials, possessing different rates of thermal expansion coefficient, are soldered or bonded together. As the component undergoes through thermal cycling, one material expands or contracts at a faster rate than the other material. This effect creates a tearing stress at the interface and leads to fractures and component failure. Copper (Cu) has a CTE of 17 ppm/ºK while the alumina (Al_2O_3) ceramic has a CTE of 6-7 ppm/ºK. The large difference of CTE between Cu and alumina causes many reliability problems in electronic power modules. The alumina provides electrical isolation between the grounded baseplate and the power devices. If a fracture develops within the alumina due to thermal cycling, a short would occur and the module would likely fail. Table 2.1 provides information on various materials used for metallization and insulative layers along with important thermal parameters associated with them.

One alternative is to use a metal-matrix composite (MMC) in place of copper.[1] MMC is composed of a ceramic or graphite matrix injected with a metal such as Aluminum (Al). Aluminum-Silicon-Carbide (AlSiC) is a MMC replacement candidate for Cu baseplates since its CTE is 7-8 ppm/ºK, which is a closer match to alumina's CTE. Matching the CTEs prevents delamination and cracking at the interface, thus leading to a more reliable product. The tradeoff of matching the CTEs of materials is a reduction in thermal capacity (thermal conductivity). The thermal conductivity of Cu is 393 W/mºK, while the thermal conductivity of AlSiC is 175-218 W/mºK. The ability to remove the proper heat during operation becomes a critical factor to consider. If the operating temperature becomes too high, the component will burn out and failure will result. Proper

analysis of the maximum operating temperature will determine whether the Cu baseplate can be replaced by a MMC baseplate.

Table 2.1. Physical Properties of Substrates and Metallization [1, 4].

Material	CTE (ppm/°K)	Thermal Conductivity (W/m°K)
AlN	3.3	170
Al_2O_3	6-7	35
AlSiC (70% SiC)	7	200-218
AlSiC (63% SiC)	7.9	175
Aluminum	24	220
Be-BeO MMC	6.1-8.7	210-230
Copper	17	393
Silicon	4.1	136
Diamond	0.8-2.0	1000-2000
Gold	14.2	317
Silver	19	429
60 Sn / 40 Pb	24.1	49.8

Figure 2.2 shows the configuration of the metallization and insulative layers using thermal spray alumina ceramic coating on an AlSiC MMC baseplate. This process holds many advantages since it reduces the number of layers. First, the AlSiC MMC baseplate does not need to be nickel coated since the insulative layer is not soldered to it. Second, the bottom layer of direct bond copper is eliminated. Third, the solder layer is not used since the insulative layer is spray coated to the baseplate. This is an advantage since the CTE of the solder layer is high, about 24 ppm/ºK. The reduction of the number of layers

will increase the reliability of the module due to the lower number of surface interfaces at which delamination or stress cracks are likely to occur.

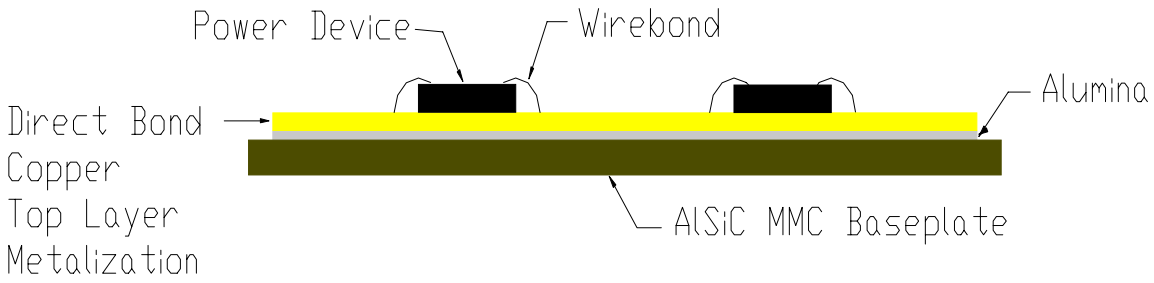

Figure 2.2. Thermal Spray Coated Power Module Baseplate.

Motorola's RF Products Division has been investigating plasma sprayed alumina as a replacement of Beryllium Oxide (BeO) ceramic substrate for a semiconductor device package.[5] BeO represents a major health hazard and using alumina as a substitute would remove the hazard. In the HOG Pak™ semiconductor package, alumina is plasma sprayed on a copper/tungsten flange. Thick film metallization is patterned on the alumina surface and semiconductor devices are attached and wirebonded to the metallization. Thin film metallization patterns can also be sputtered on the alumina.

2.3 Conclusion

Thermal sprayed alumina ceramic is providing new options in semiconductor discrete devices and their electronic packaging. Thermal spray alumina decreases the number of metallization layers within the device reducing the possibility of CTE mismatch cracking and delamination. Production costs can be lower due to the elimination of production steps such as nickel coating the baseplate and soldering the baseplate to the DBC substrate. Studies have shown that alternate MMC baseplates can be used in place of copper while still providing ample heat dissipation.[1] Thermal spray alumina ceramic offers an alternative that allows electronic power modules to be manufactured to provide a higher reliability product.

CHAPTER 3

THERMAL SPRAY

3.1 Technique Concept

This chapter is concerned with the topic of thermal spray. Thermal Spray is a group of processes which feed metallic, ceramic, cermet, and some polymeric materials in the form of powder, wire or rod into a torch or gun where they are heated to near or somewhat above their melting point.[3] The molten droplets of material are accelerated in a gas stream and impinged upon the surface to be coated. The droplets flow into thin lamellar particles. Once the particles adhere to the surface, they cool, shrinking and interlocking as they solidify. A desired thickness is obtained by making several passes applying layer upon layer. The surface intended to be coated needs to be roughened to promote the adhesion process.

To prepare a substrate to be spray coated, it must first be properly processed. The substrate needs to be cleaned to remove any surface contaminants. Aqueous detergents and alkaline cleaners, used in conjunction with ultrasonic agitation, are used to remove surface contaminants. Grit blasting will roughen the cleaned surface and increase its coefficient of friction allowing the thermal spray particles to adhere.

3.2 Microstructure

Thermal spray coatings consist of many layers of thin, overlapping, essentially lamellar particles. As the material is introduced into the spray gun, the particles receive thermal energy from the high velocity gas and melt into droplets. The droplets receive kinetic energy from the high velocity gas and move towards the target where they impinge upon the surface like a “splat”. On contact with the target surface, the droplets

transfer thermal energy to the substrate through conduction and revert back to a solid. As they cool, they shrink, inducing a mechanical interlocking structure. Quench rates have been estimated to be 10^4 to 10^6 ºK/s for ceramics and 10^6 to 10^8 ºK/s for metallics.

The structure of a thermal spray coating tends to very porous. Porosities of High-Velocity Oxyfuel (HVOF) coatings are less than 2%, while porosities resulting from plasma spray coatings are expected to be in the range of 5 to 30%.[6] The porosities of flame sprayed coatings may exceed 15%.[3] The degree of porosity is dependent on the melted state of the sprayed particle. The melted state of the particle determines the ability to deform on impact leading to the bonding structure.[7] In evaluating dielectric breakdown, porosity plays a major role in the amount of voltage an insulative layer can withstand. If the coatings are exposed to a humid environment, moisture can accumulate within the structure voids leading to a lower breakdown voltage. This situation can be prevented controlling the environment during processing and then hermetically sealing the package. A second consideration that cannot be changed is the fact that the voids contain air, and air would have a much lower breakdown voltage than the insulative material.

3.3 Plasma Spray

Low temperatures restricted early forms of thermal spray since they were produced by an oxyacetylene flame or an electric arc. Materials with melting points of 2700 °C and higher cannot be sprayed. Attempts to extend the temperature range of the heat source lead to the development of plasma spraying. Plasma is the highly ionized state of mass, consisting of molecules, atoms, ions, electrons, and light quantums.[8,9] Plasma arc torches began to be experimented with about 1958. There are two basic types of plasma torches and they are determined by the arrangement of the electrodes between which the electric plasma burns. A non-transferred arc, shown in Figure 3.1, is when the arc burns between the negative cathode and the positive anode within the nozzle. A transferred arc, shown in Figure 3.2, is when the positive pole is transferred to an external

conductive material located in front of the nozzle and is usually employed in welding, surfacing, or metal cutting.

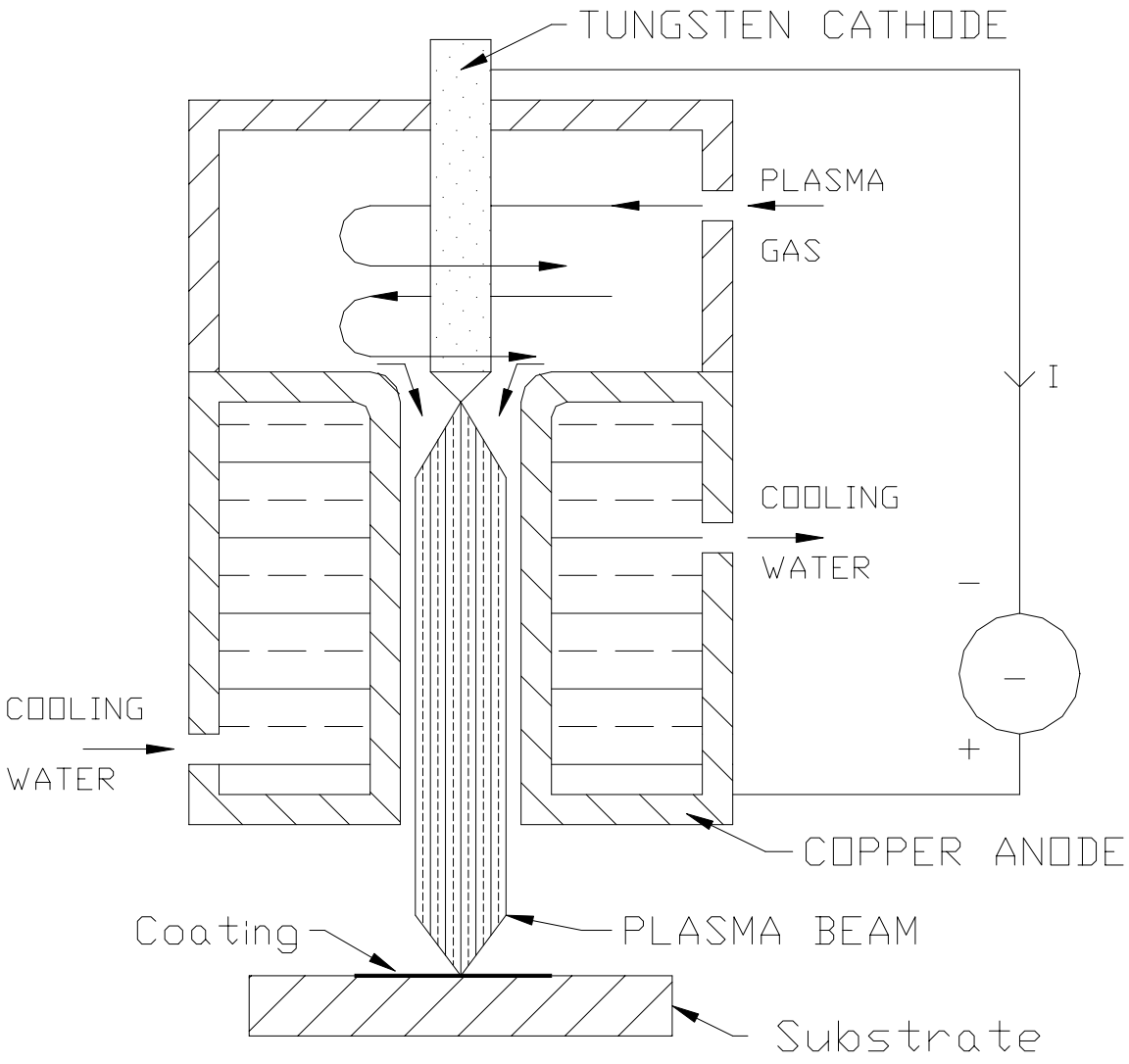

Figure 3.1. Non-transferred Arc Plasma Beam [8].

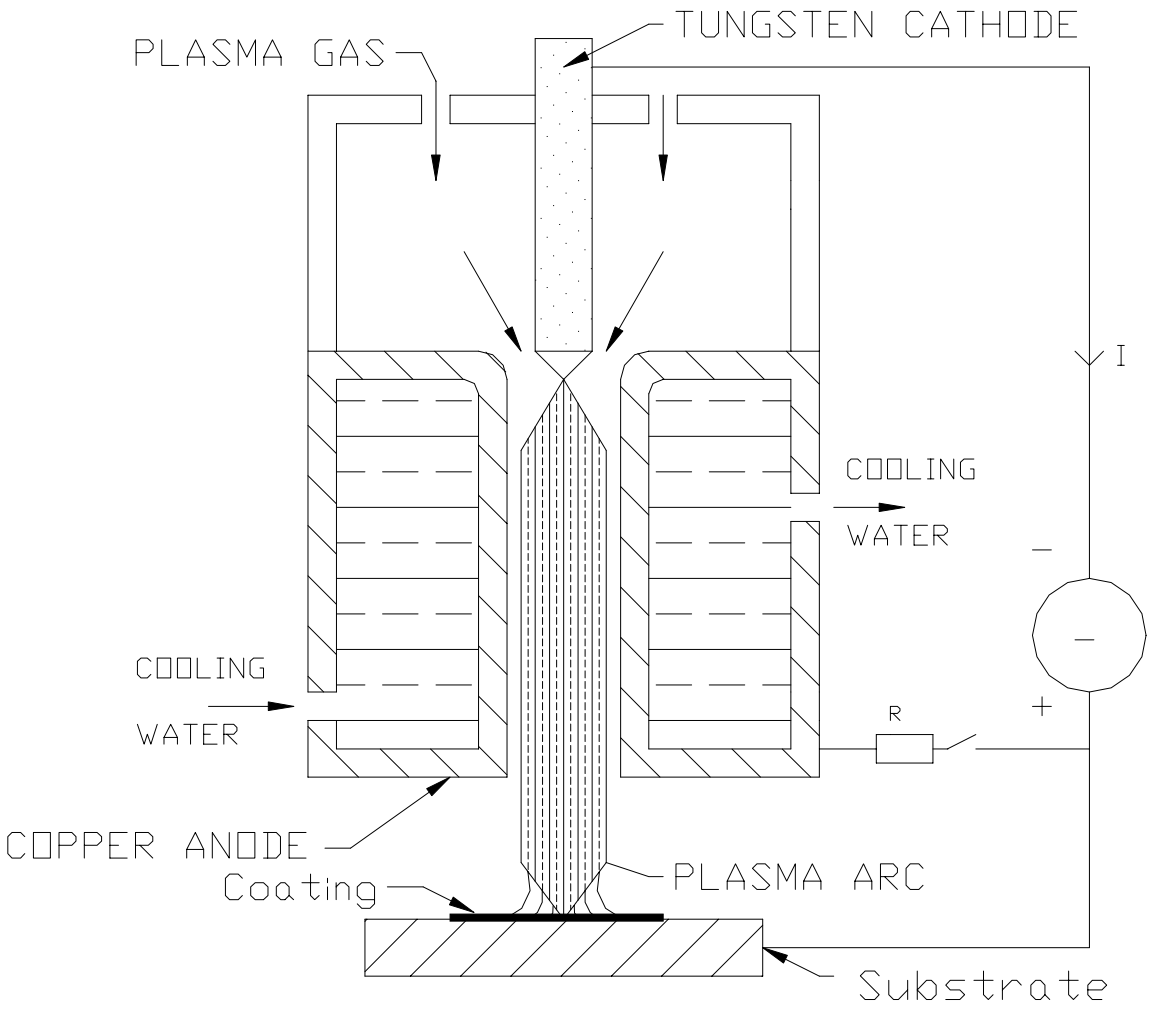

Figure 3.2. Transferred Plasma Arc [8].

Plasma gases used for thermal spraying include Argon (Ar), Helium (He), Hydrogen (H_2), and Nitrogen (N_2). This criteria divides plasma forming gases into two groups: one-atom and two-atom gases. Argon and helium make up the first group, while

nitrogen and hydrogen form the second group. The basic physical and chemical characteristics of applied plasma-forming gases are tabulated in Table 3.1. The objective of the plasma forming gases is two-fold; first to form the plasma, and second to protect the electrodes from oxidation and aid in their cooling. Plasma gases are selected on the basis of the desired temperature and the velocity of the plasma beam and the degree of inertness in the sprayed material and substrate. The formation process of plasma from a two-atom gas differs from the formation process of a one-atom gas. The difference is that the ionization of a two-atom gas starts after dissociation of its molecules. Hydrogen dissociates by 90% at 5000 ºK and nitrogen dissociates at a temperature of at about 8500 ºK.

Table 3.1. Physical and chemical characteristics of plasma gases [8].

Characteristic	Unit	Argon	Helium	Nitrogen	Hydrogen
Relative molecular weight		39.44	4.0002	28.016	2.0156
Specific Weight at 0 ºC and 101.32 Pa	($kg*m^{-3}$)	1.783	0.1785	1.2505	0.0898
Specific thermal capacity C_p at 20 ºC	($kJ*kg^{-1}K^{-1}$)	0.511	5.233	1.046	14.268
Coefficient of Thermal Expansion (CTE) at 0 ºC	($W*m^{-1}K^{-1}$)	0.06133	0.14363	0.02386	0.17543
Ionization potential					
one-stage	(V)	15.7	24.05	14.5	13.5
two-stage	(V)	27.5	54.1	29.4	-
Temperature	(K)	14000	20000	7300	5100
Arc voltage	(V)	40	47	60	62
Arc input	(kW)		50	65	120
Coefficient of energy utilization for gas heating	(%)	40	48	60	80

Nitrogen dissociation starts at 5000 ºK and is 95% complete at 9000 ºK. Ionization of nitrogen atoms start at 8000 ºK, it is 50% complete at 15000 ºK, 95% complete at 20000 ºK, and 98% at 22000 ºK. Due to a higher enthalpy, nitrogen plasma above 7000 ºK, contains greater heat volume than the other gases at the same temperature. This leads to greater torch-work distances when using nitrogen compared to argon. The nitrogen used must be free of oxygen otherwise poisonous nitrogen oxide is formed and electrode oxidation may occur. Figure 3.3 profiles the temperature distribution on nitrogen plasma.

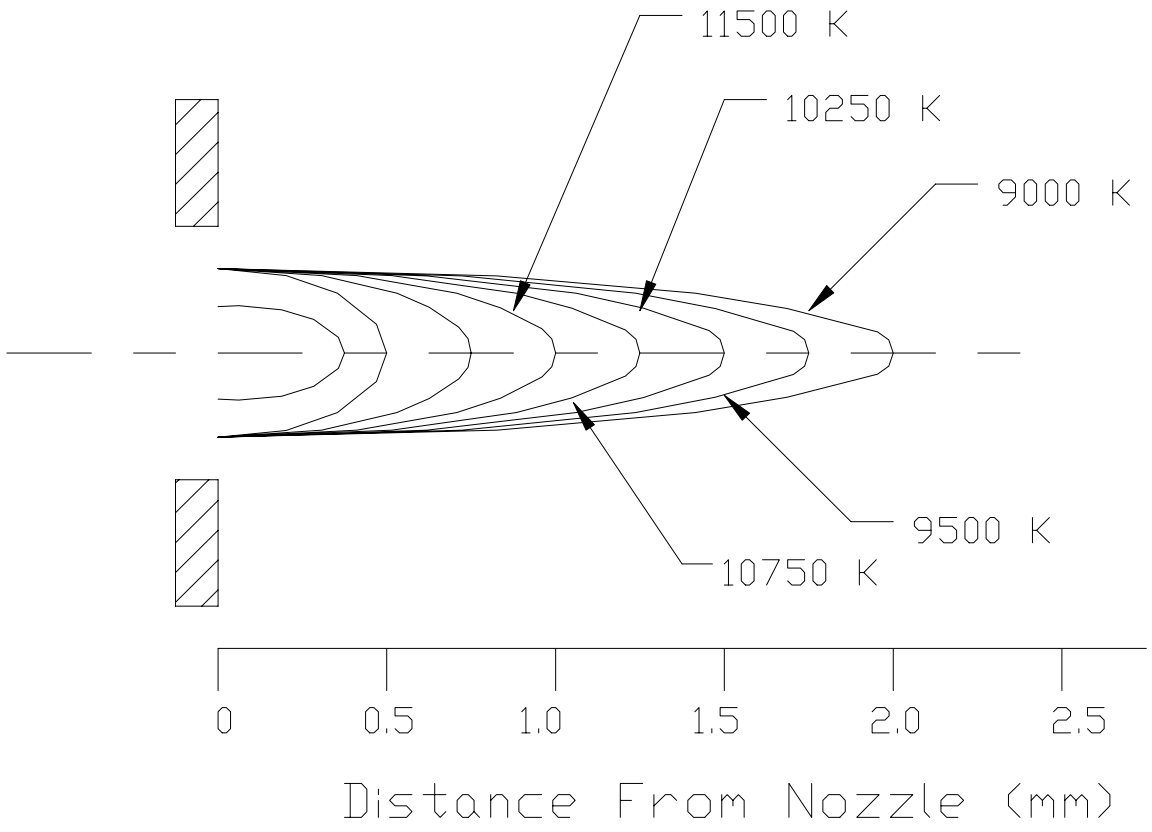

Figure 3.3. Distribution of Temperatures in Nitrogen Plasma [8].

Hydrogen dissociation starts at 2000 ºK and is completed at 6000 ºK. Hydrogen dissociation requires less energy than the dissociation of nitrogen and hydrogen has the highest thermal conductivity of plasma gases. Although hydrogen plasma requires a very high arc voltage, the temperature of the plasma is lower than other plasma gases, around

5100 ºK. When using hydrogen, one has to be cautious since the hydrogen can mix with oxygen and form an explosive mixture.

Argon and helium do not possess a diatomic structure allowing them to become ionized without a dissociation process. Ionization of argon starts at 9000 ºK and is completed at 22000 ºK. Argon is the preferred plasma gas since it transfers to a plasma state easier than other gases and also provides a stable electric arc while requiring a lower working voltage. Argon plasma also achieves a high temperature when compared to other plasmas. Helium plasma obtains a high temperature with excellent thermal conductivity but it is a very expensive and precious gas. Since argon and helium do not dissociate, their beam is very bright, short and constricted. This facilitates local deposit of the spraying layer, allowing higher spraying efficiency. Figure 3.4 profiles the temperature distribution on argon plasma. Standard spray conditions using argon with various sprayed materials are summarized in Table 3.3.

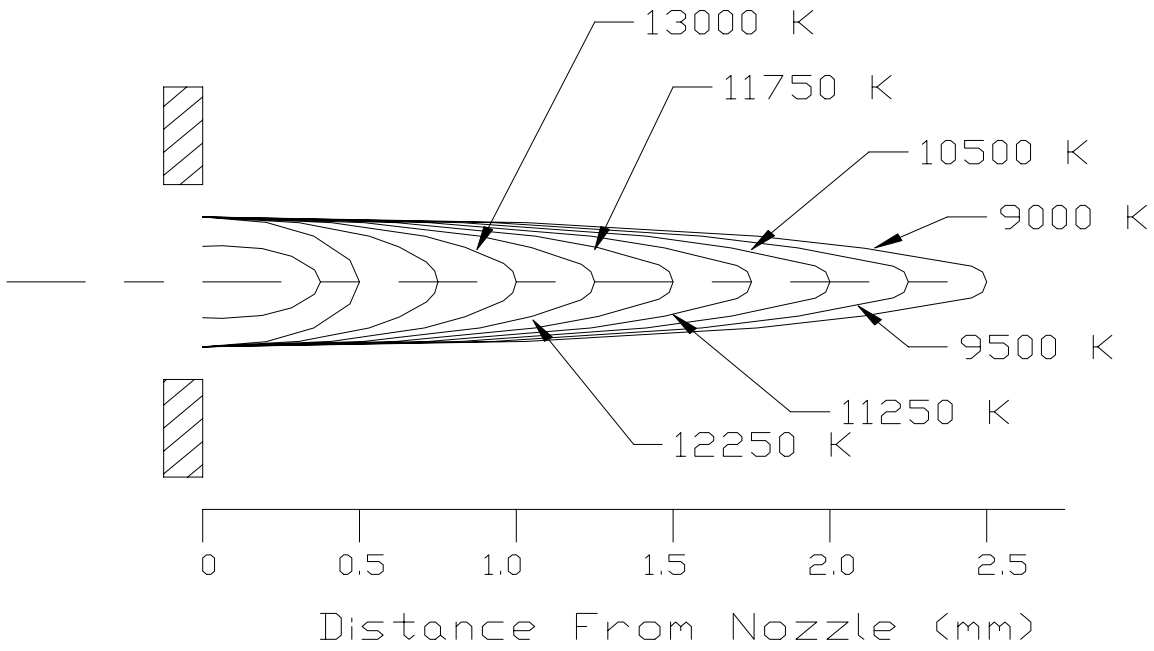

Figure 3.4. Distribution of Temperatures in Argon Plasma [8].

Temperature is an important parameter to be considered since the coating material needs to be melted when it contacts the target. This allows the particle to conform to the deformations of the underlying surface maximizing surface contact and minimizing voids. This also leads to higher thermal conductivity. Table 3.2 shows temperature schemes that can be obtained by varying the gas flow rate and the electric arc.

Table 3.2. Mean and Maximum Temperatures of Argon and Nitrogen Plasmas [8].

Output (kW)	Temperature (K)	Gas flow rate					
		15 l/min		30 l/min		60 l/min	
		Argon	Nitrogen	Argon	Nitrogen	Argon	Nitrogen
5	T max	11400	--	11750	--	12000	--
	T mean	8850	--	5600	--	3000	--
10	T max	--	10900	12700	11040	13000	10540
	T mean	10750	7100	9600	6250	6600	5550
15	T max	--	12370	14500	11990	14400	12180
	T mean	12000	7550	11000	6700	8750	5950
20	T max	--	13830	--	14790	--	13100
	T mean	--	8250	--	7100	--	6200

Table 3.3. Standard Spraying Conditions [10].

Material	Arc Gas Flow rate m^3/hr	Powder Gas Flow Rate m^3/hr	Distance Mm	Hopper Setting	Feed Rate g/min	Efficiency %
Alumina	1.0	0.34	40-50	11	20	85
Aluminum	1.5	0.27	75	8	19	95
Al Bronze	1.4	0.29	75	10	64	85
Chromium	1.4	0.31	50-75	10	78	87
Cr Oxide	0.8	0.24	50	10	34	80
Copper	1.5	0.31	75	8	73	77
Nickel	1.4	0.27	75	6	75	80
Silicon	1.4	0.31	50	2	16	51
Titanium	1.5	0.24	50	6	23	90
Zirconia	1.5	0.31	40	8	25	64
Arc gas: argon Current: 500 amps						

3.4 High-Velocity Oxyfuel (HVOF) Thermal Spray

High-velocity oxyfuel thermal spray is a technique where a combustible fuel, usually propane, propylene, MAPP, or hydrogen, is mixed with oxygen and burned in a chamber. The products of combustion are allowed to expand through a nozzle where the gas velocities become supersonic. A coating powder is introduced in the nozzle where it absorbs thermal and kinetic energy allowing the powder to melt and move towards the target surface. Figure 3.5 illustrates the HVOF thermal spray technique.

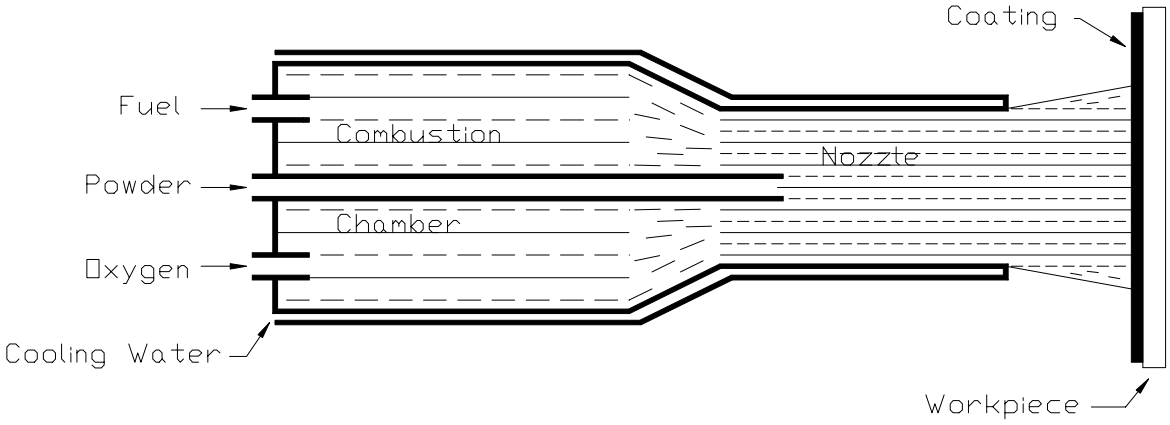

Figure 3.5. High-Velocity Oxyfuel Process [3].

HVOF processes can produce coatings with a higher density than when using plasma spray processes. This characteristic would lead to a higher breakdown voltage rating due to less porosity in the coating allowing air and moisture to be within the coating. Virtually, any metallic or cermet material can be coated using the HVOF process. When coating ceramics, an acetylene fuel is required in order to reach the high melting point. Ceramics can be coated using a new spray gun trademarked TOP GUN™. The main feature of this spray gun is the oxygen being injected at a high pressure through a number of tubes into the combustion chamber, while the fuel gas is aspirated into the oxygen stream and is mixed with oxygen before the gases enter the combustion chamber. The advantage of this gun is that the fuel gas needs not to be injected at a high pressure,

therefore acetylene can be used as a fuel gas as well as propane, propylene or hydrogen. Typical settings for the gas pressures at the console are 0.95 bar acetylene and 4.0 bar oxygen or 1.5 bar propane and 6.4 bar oxygen. Studies have shown that spraying alumina with propane results in a porous coating due to the temperature not being high enough to melt the alumina particles while using acetylene fuel melted the alumina and resulted in denser coatings.[11] The ability to apply ceramics allows the HVOF process to be used to coat electric isolation layers which is a study conducted in this thesis. Since the thermal energy comes from oxygen and fuel combustion, no electricity is needed. This characteristic eliminates the danger of working with high voltages and currents.

Higher density of the coatings is partly attributed to the high velocity obtained by the sprayed particles. Spray gun design plays an important role in determining the velocity of coating particles as they impinge on the surface of the substrate. To achieve maximum particle velocity, it is critical to maximize velocity of the gas within the barrel since the particles reach only a portion of the gas velocity. As the gas exits the gun barrel, the velocity decreases as it progresses further away. As the coating particles are introduced into the gas stream, they receive thermal and kinetic energy from the gas stream. The particles melt into droplets while accelerating rapidly within the gun barrel. On exiting the barrel, the particles continue to slowly accelerate until their velocity matches the decreasing gas velocity. After this point, the velocity of the particles began to decrease also. Peak velocity of 5 μm alumina occurs around 5 cm from the nozzle with a velocity of approximately 1400 m/s.[12] Lengthening the barrel will increase particle velocity due to the particles accelerating within the barrel while the gas stream velocity is relatively constant until exiting the barrel. Optimum particle velocity and the soft melt particle temperature will determine the quality of the coating. The coating particle needs to be softly melted and traveling at sufficient velocity to cause it to form a splat when it contacts the substrate surface.

3.5 Conclusion

Thermal spray coatings can be used to provide an electric isolation layer. Two types of thermal spray processes, plasma spray and high-velocity oxyfuel (HVOF), provide high enough temperatures in order to spray ceramic coatings. Alumina is a ceramic that provides electrical isolation and can be sprayed using both processes. Plasma sprayed alumina has been used by Ford Motor Company in Ypsilanti, Michigan since 1990 to coat the control plate of an alternator. This provides an electrical insulator between the positive and negative diodes.[13] Other applications are being developed throughout the electronic industry.

Plasma spray coatings represent the majority of thermal sprayed ceramics today. The process generally uses argon as the plasma gas through a non-transferred arc system. High particle velocities need to be achieved otherwise the coating will result in a porous composition.[14] Porosity's of 5 to 30% can occur using plasma spraying. The voids of a porous coating allow trapped air and moisture to lower the dielectric breakdown rating. Good particle melting and adequate velocity when the particle impinges on the substrate surface yields coatings with a reasonable porosity.

HVOF thermal spray coatings are produced when powder is introduced axially into a gas stream of combustion chamber products resulting from oxygen and fuel igniting. To spray alumina ceramic coatings, the fuel used has to be acetylene in order to produce high enough temperatures. While being accelerated, the spray particles melt, and they are bombarded onto the substrate surface. The droplets solidify upon contact with the substrate producing a lamellar structure. The particle velocity achieved with the HVOF process is higher than plasma spraying and leads to the tendency that HVOF coatings have a lower porosity, as low as 2%. Spray gun design is important to provide optimal pressures, barrel velocities, precise powder injection points allowing desired particle acceleration in the barrel leading to high quality coatings. With new developments in the Top Gun ™ spray process, HVOF thermal spray coatings will be used in an increasing number of electronic applications in the future. The ability to provide electric isolation with thermal sprayed alumina ceramic will supply the need for

improving old technologies and for new technologies to be developed. The amount of electric isolation provided can be determined by dielectric breakdown voltage test.

CHAPTER 4

DIELECTRIC BREAKDOWN VOLTAGE TEST

4.1 Introduction

This chapter is concerned with testing the dielectric breakdown voltage, or dielectric strength, of solid electrical insulating materials under direct-voltage stress. This test method measures the ability of a material to resist the flow of current in the presence of an electric field. The energy bands of an insulator is shown in Figure 4.1. The valance band of an insulator is full of electrons while the conduction band is essentially empty of these carriers.

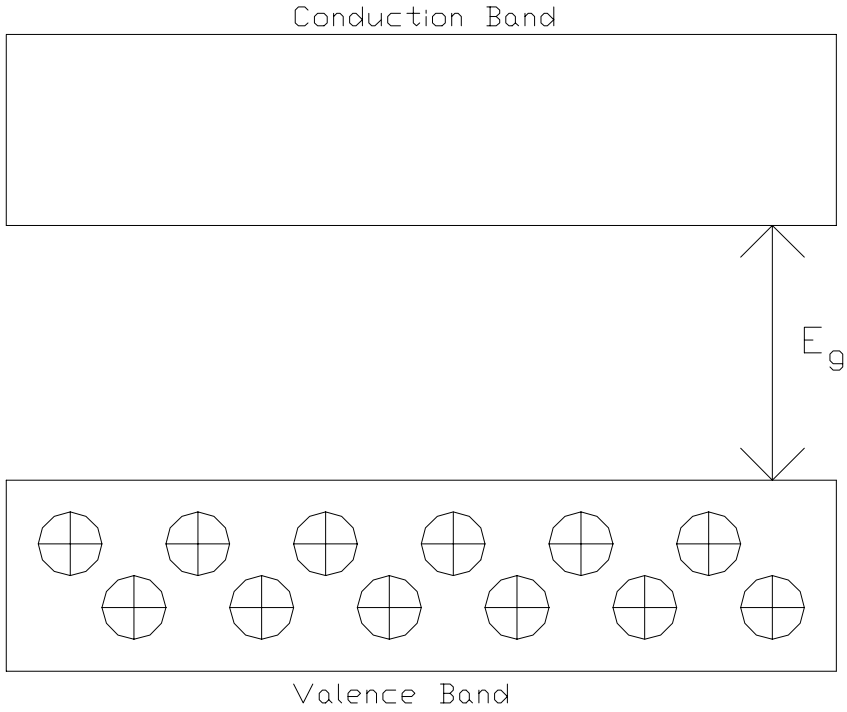

Figure 4.1. Energy Band Diagram of Insulator [15]

The bandgap energy, E_g, of an insulator is usually on the order of 3.5 to 6 eV or larger.[15,16] This energy level allows the valance band to remain full of electrons and the conduction band to remain empty at room temperature. Even though the electrons at room temperature have gained thermal energy, they still do not have enough energy to cross the bandgap. As an electric potential is applied across an insulative material, the electrons gain energy and move toward the higher energy states within the conduction band. As the electric potential is increased, more and more electrons make their way to the conduction band and current starts to flow. This current is referred to as leakage current and is usually small in the order of microamps. As the voltage is increased further, the electrons become highly excited and start colliding into other atoms, knocking them and basically freeing carriers, allowing them to aid in electrical conduction. Eventually, the collisions of the electrons produce an avalanche effect, allowing the leakage current to explode in magnitude, virtually creating a short circuit.

4.2 Technique

The standard test method for dielectric breakdown voltage and dielectric strength of solid electrical insulating materials under direct-voltage stress is defined by the American Society for Testing and Materials (ASTM) in D3755-86 (Reapproved 1995).[17] The specification states that the specimen is to be held in a properly designed electrode system and electrically stressed by the application of an increasing direct voltage until internal breakdown occurs. The test voltage is applied at a uniform increase rate and is provided by a high-voltage supply of adequate current capacity and regulation. The ripple of the filtered output voltage should be less than 1%. Voltage control is necessary to provide a linear rate-of-rise in voltage throughout the test. A voltmeter is needed to observe the magnitude to the voltage being applied to the device under test (DUT) and should not have an error greater than $\pm$2%. The electrodes are selected to provide adequate electrical contact. One electrode is set to ground while the other electrode is energized with a direct-voltage. A test chamber is necessary in which to perform the desired breakdown tests and should be grounded to prevent accidental

electrocutions. Safety precautions are extremely important since lethal voltages are present during breakdown tests. When a direct-voltage test has been applied to the test specimen, both the specimen and the power supply can remain charged after the test voltage source has been de-energized. Section 7.4 states a manual grounding stick must be used to completely discharge the test specimen and the power supply after the test, prior to handling either of them.

While the breakdown test is being performed, the voltage is increased until the dielectric can no longer provide insulation between the electrodes and the current flows freely. At the initial onset of voltage between the electrodes, a small amount of leakage current can be present. The leakage current can increase with an increase in voltage until the breakdown voltage is reached and the current increases sharply. A circuit breaker is advisable to protect the power supply from the current spike produced when the dielectric breakdown creates a virtual short circuit.

The geometry of the test specimen is an important characteristic that needs to be taken into consideration. The DUT needs to be of sufficient area to prevent flashover. Flashover is a disruptive electrical discharge at the surface of electrical insulation or in the surrounding medium, which may or may not cause permanent damage to the insulation.[18] Thick specimens need to be tested in an insulating fluid due to the fact that air breaks down at 76 volts/mil and it would be easier for the electric current to flashover through the air and around the DUT. Dielectric mineral oils have breakdown voltages over 26kV and are typical of insulating fluids found in transformers, circuit breakers, capacitors, or cables.[19]

Conditioning of the test specimen is necessary since moisture will affect the dielectric strength. ASTM specification D618-95, “Standard Practice for Conditioning Plastics and Electrical Insulating Materials for Testing”, specifies methods of heating the test specimen to remove unwanted humidity. An example conditioning is 24/125:T-27 which translates into condition for 24 hours at 125 ºC and test at 27 ºC, room temperature.[20]

4.3 Test Apparatus

The test apparatus needed to perform direct-voltage breakdown tests consists of a power supply, test chamber, electrodes, voltmeter, and voltage control. The configuration shown in Figure 4.2 was used to test direct-voltage dielectric breakdown. In this setup, a personal computer is connected to a high voltage power supply by an IEEE-488 GPIB interface buss. This allows the computer program Labview™ to control the operation of the power supply. The baseplate (DUT) is placed in a grounded test container so that the positive electrode makes adequate electrical contact with it. The power supply is ground to complete the electrical circuit.

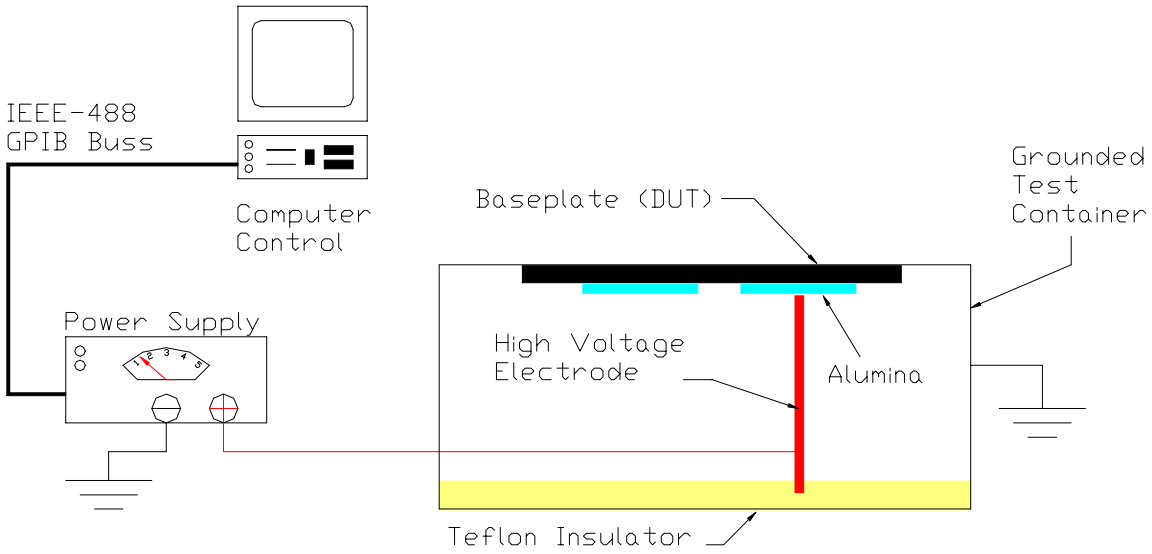

Figure 4.2. Dielectric Breakdown Test Apparatus.

The test apparatus shown in Figure 4.3 is used to measure direct-voltage leakage current at voltages below the breakdown level. In this setup, a personal computer is connected to a high voltage power supply by an IEEE-488 GPIB interface buss. This allows the computer program Labview™ to control the operation of the power supply. The baseplate (DUT) is placed on an insulative layer of Teflon™ in a grounded test container so that the positive electrode makes adequate electrical contact with it. A resistor network is connected from the insulated baseplate to the ground test container. A digital multimeter is connected across the resistor and measures the voltage drop across it. The leakage current in the circuit is obtained from ohm's law: I = V/R. An electrical schematic of the direct-voltage leakage test apparatus is shown in Figure 4.4.

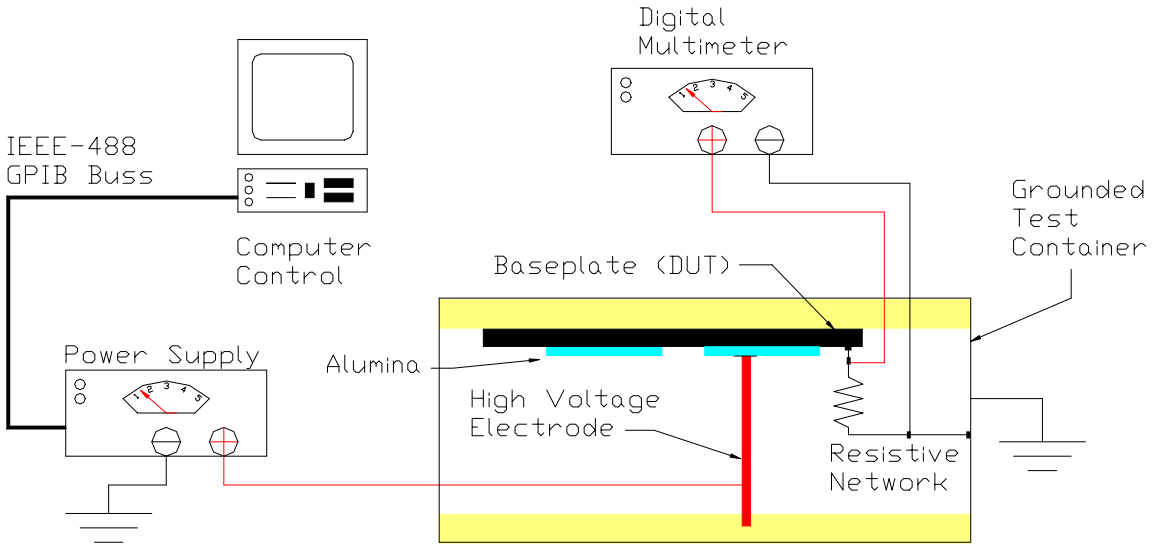

Figure 4.3. Leakage Current Test Apparatus.

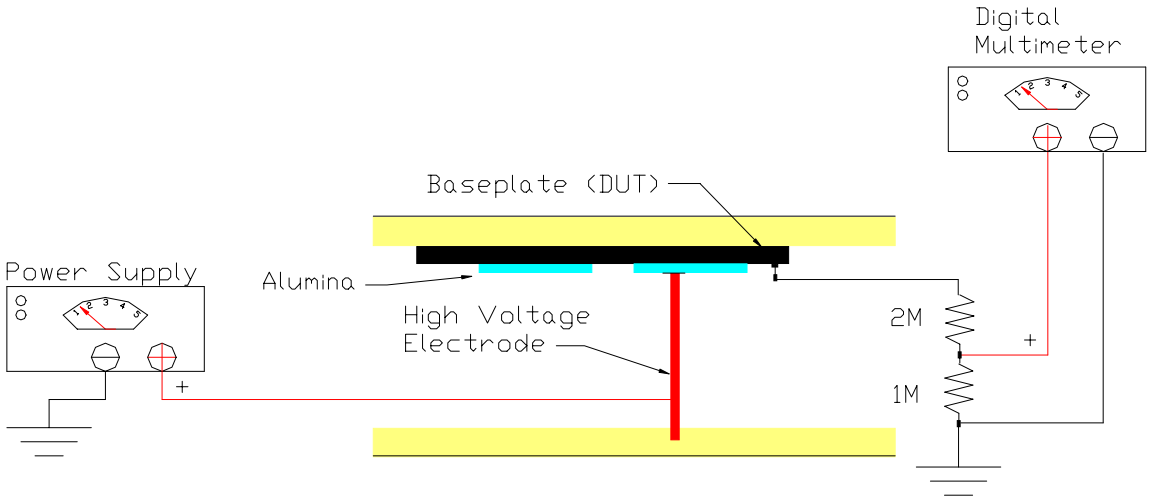

Figure 4.4. Leakage Current Test Apparatus Schematic.

The purpose of using the configuration of Figure 4.4 to test for leakage current is to amplify the resolution of the current. Precision resistors of 1 MΩ and 2 MΩ are placed in series with the baseplate, which is insulated and floating with reference to ground. The positive electrode from the power supply is placed in contact with the alumina ceramic layer. Both the power supply and the 1 MΩ resistor are connected to ground to complete the circuit. A digital multimeter is connected across the 1 MΩ resistor to measure the voltage drop across it. Regardless of the leakage current magnitude flowing through the alumina, it also passes through the 1 MΩ resistor and produces a voltage drop. Backwards induction allows the voltage read on the digital multimeter to be divided by the resistance thus giving the leakage current. Since the resistance of the alumina ceramic is several orders of magnitude higher than the two resistors, very little error is introduced. The digital multimeter can measure 0.1 mV. By dividing this value by a resistance of 1 MΩ, this test apparatus can measure a leakage current with a resolution of 0.1 nA.

4.4 Computer Control

Labview™ is computer software that allows a personal computer to control test equipment. A Labview™ program instructs the power supply to step up the voltage and then records the current in the circuit. Communication between the computer and lab instruments is over an IEEE-488 GPIB interface buss. Labview™ is a graphical software program that allows the user to construct a control program using graphical building blocks.[21] Figure 4.5 shows a sample screen of the program HPOWER1.VI and appendix A includes complete documentation of this program. User inputs include starting voltage, step voltage, stop voltage, step time increment, and data storage file. The data file can be imported into a Microsoft Excel™ spreadsheet to be tabulated and charted.

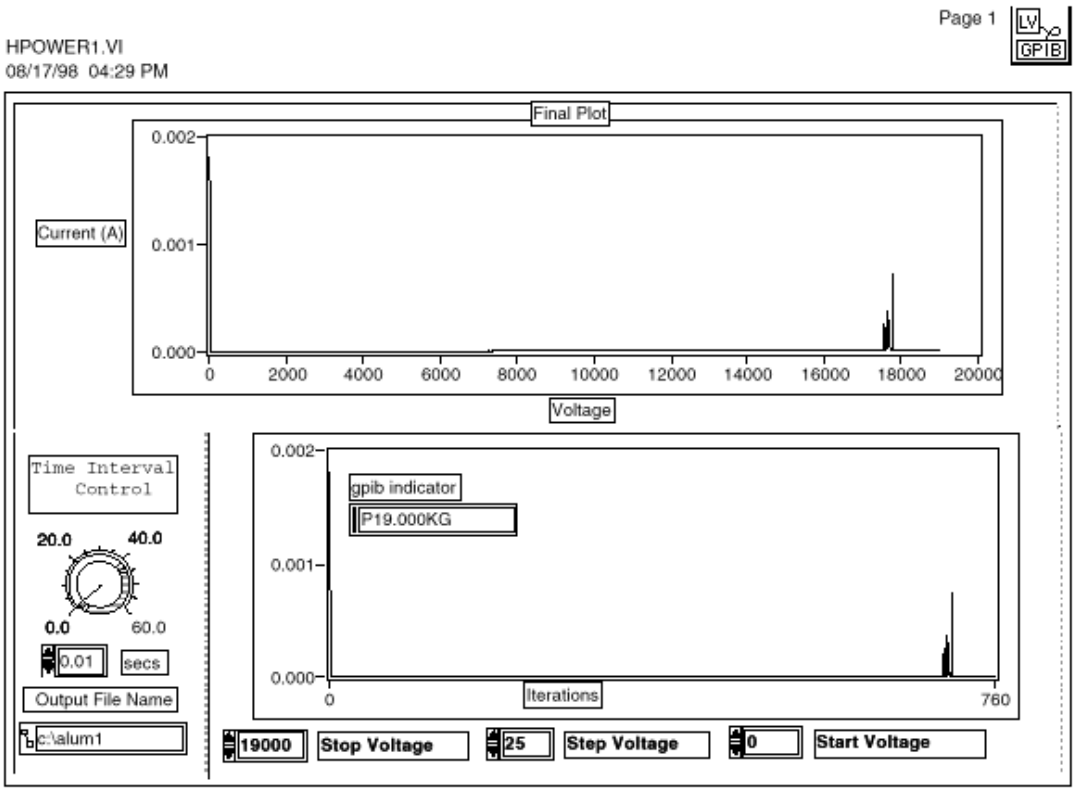

Figure 4.5. Breakdown of 25 mil thick alumina substrate.

4.5 Conclusion

The dielectric strength of the insulative layer is an important aspect in electronic power modules. Currently, power modules operate at extremely high voltages and the insulative layer prevents a short to ground. If the operating voltage is above the dielectric breakdown voltage of the insulative layer, a short to ground occurs and the power module will be destroyed. Adequate testing of dielectric strength of the insulative layer insures an acceptable reliability in manufactured electronic power modules. ASTM sets the standards for the testing of dielectric breakdown voltage so that industry ratings can be assessed across the industry.

The amount of leakage current present at operating voltages is an important characteristic since this leakage current adds to the power dissipated and becomes heat that has to be removed. Excessive leakage current can make the power module operate at too high a temperature leading to component failure and lowering the modules reliability.

Labview™ programs aid in the testing of direct-voltage dielectric breakdown voltage and direct-voltage leakage current by controlling the instrumentation performing the tests. Programs can be developed to perform special controlling functions as well as special data handling and manipulation functions. Labview™ uses an IEEE-488 GPIB interface buss which is common on most lab testing equipment.

CHAPTER 5

VERIFICATION AND VALIDATION OF TEST RESULTS

5.1 Introduction

This chapter presents the data collected from direct-voltage breakdown tests and direct-voltage leakage current tests. Four lots of thermal spray alumina coupons were obtained from Lanxide, Inc., for testing. Lots one and two are manufactured using the plasma spray technique and lots three and four are manufactured using the HVOF process. Lots one and three are rated by the manufacture to have a minimum dielectric strength of 3000 V and lots two and four are rated to have a minimum dielectric strength of 5000 V. Cross-sectional pictures of the material layers are obtained using scanned electron microscopy (SEM) as well as elemental analysis of the materials layers using EDAX. Isolation layer thickness is measured using a dead-weight dial type bench micrometer (manual).[22] Thickness measurements are detailed in appendix B.

5.2 Lot 1 Plasma Spray Alumina 3000 V

Lot 1 consists of four coupons manufactured using plasma spray technology and rated to have a minimum dielectric strength of 3000 V. The thickness of the alumina isolation layer is measured to be 18 - 20 mils. Figure 5.1 illustrates a graphical presentation of direct-voltage dielectric breakdown voltages tests performed on Lot 1 Coupons 1A, 2A, and 3A. Coupon 1A is tested “as shipped” from the manufacturer, Coupon 2A is tested after being conditioned for 24 hours at 125 ºC, and Coupon 3A is tested after being conditioned for 24 hours at 200 ºC. “As shipped” means the coupon has not been conditioned to remove trapped moisture. Conditioning is defined in Section 4.2 as the process used to remove trapped moisture. Figure 5.1 illustrates the dielectric breakdown voltage rating is met with three different conditioning scenarios. Figure 5.2 shows the results of a direct-voltage leakage current test perform on coupon 4A with

three different scenarios. Coupon 4A is tested as shipped, conditioned 24 hours at 125 ºC, and then conditioned for an additional 24 hours at 200 ºC. Figure 5.2 illustrates the effect of trapped moisture on leakage current. Note that the same coupon is tested using three different conditioning scenarios.

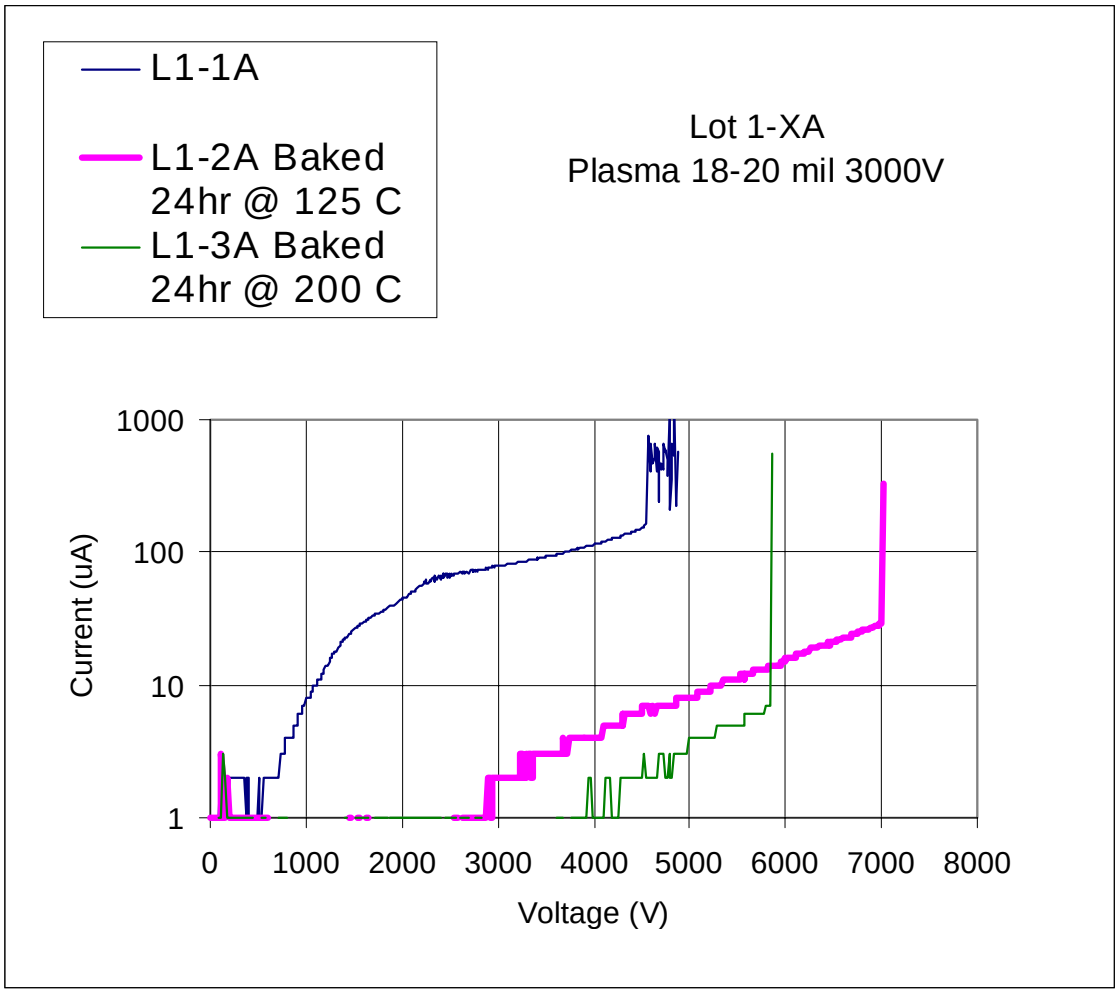

Figure 5.1. Dielectric Breakdown Voltage Results Lot 1-xA.

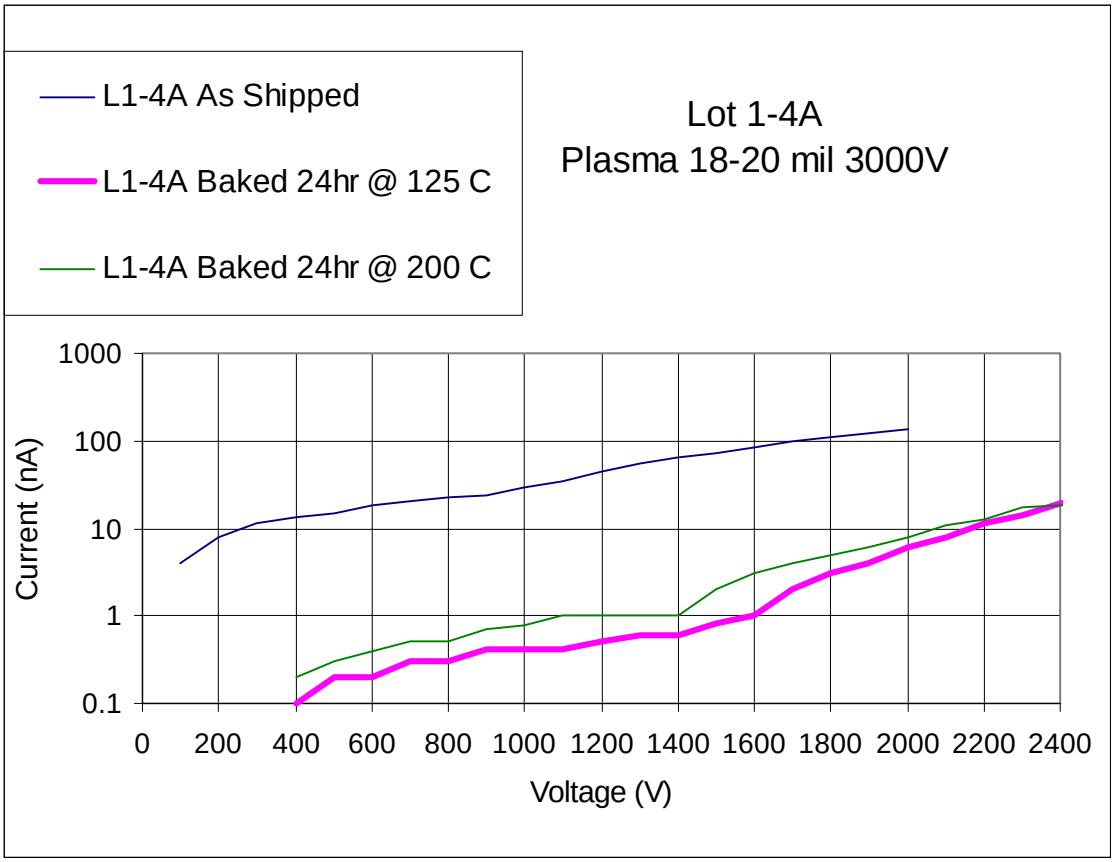

Figure 5.2. Lot 1-4A Dielectric Leakage Current Test.

Figure 5.3 shows a graphical presentation of direct-voltage dielectric breakdown voltages tests performed on Lot 1 Coupons 1B, 2B, and 3B. Coupon 1B is tested as shipped from the manufacture, Coupon 2B is tested after being conditioned for 24 hours at 125 ºC, and coupon 3B is tested after being conditioned for 24 hours at 200 ºC. Figure 5.3 illustrates that all three coupons tested meet the manufactured dielectric strength rating and moisture affects both the leakage current and the dielectric strength.

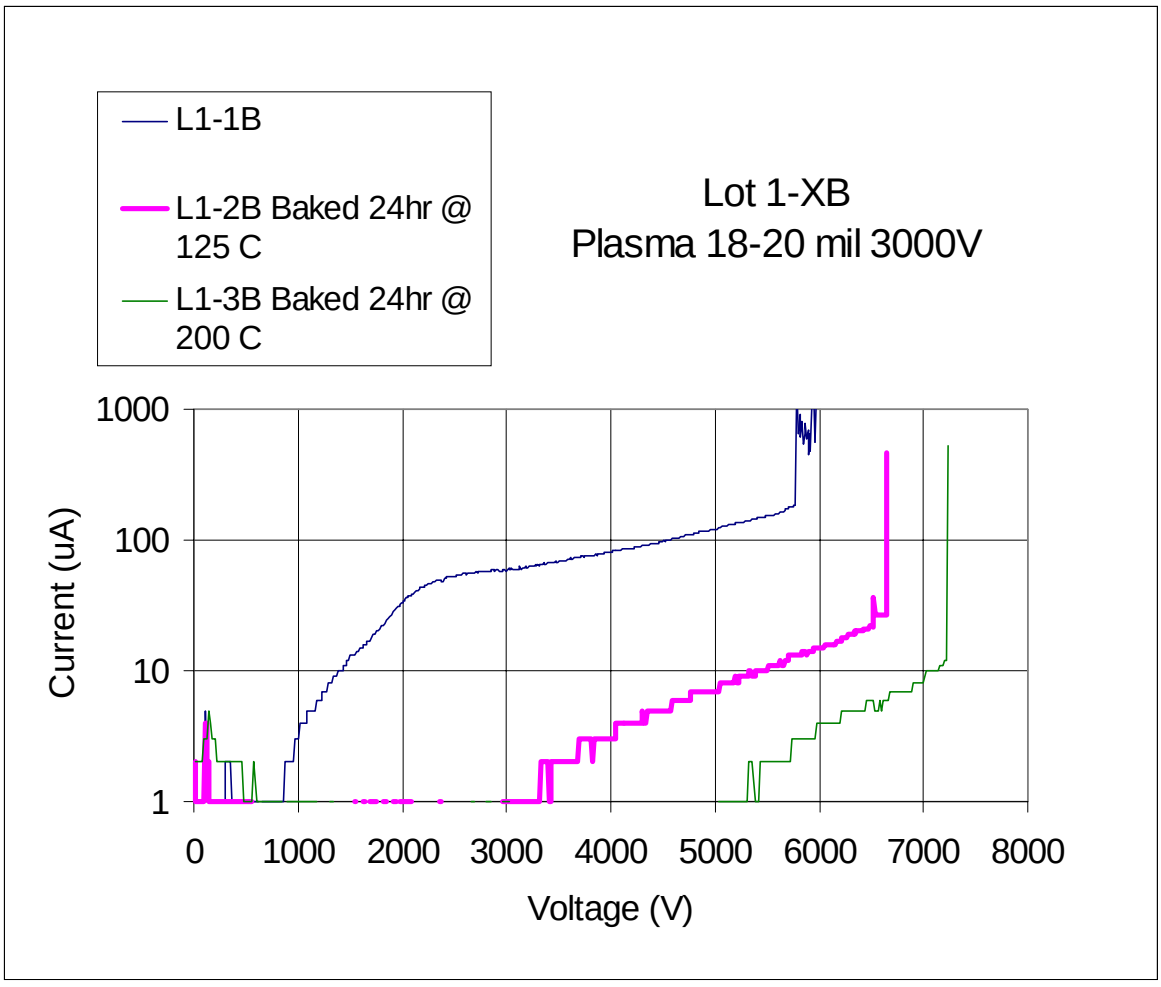

Figure 5.3. Dielectric Breakdown Voltage Results Lot 1-xB.

The interface between the AlSiC MMC baseplate and the alumina ceramic insulative layer is shown in Figure 5.4. The picture is the cross-section of Lot 1-1A using a SEM with backed scanned electron enhancement. As plasma sprayed alumina particles impinge the surface of the substrate, they conform to the substrate surface creating a mechanical bond. The lack of voids and cracks, not seen in the cross-sectional view, implies excellent adhesion and good mechanical bonding. The picture also illustrates the surface roughness of the plasma sprayed alumina. This can lead to problems in bonding a layer of metallization to the alumina. The alumina may need to be polished, mechanically or chemically, to prepare a suitable bonding surface.

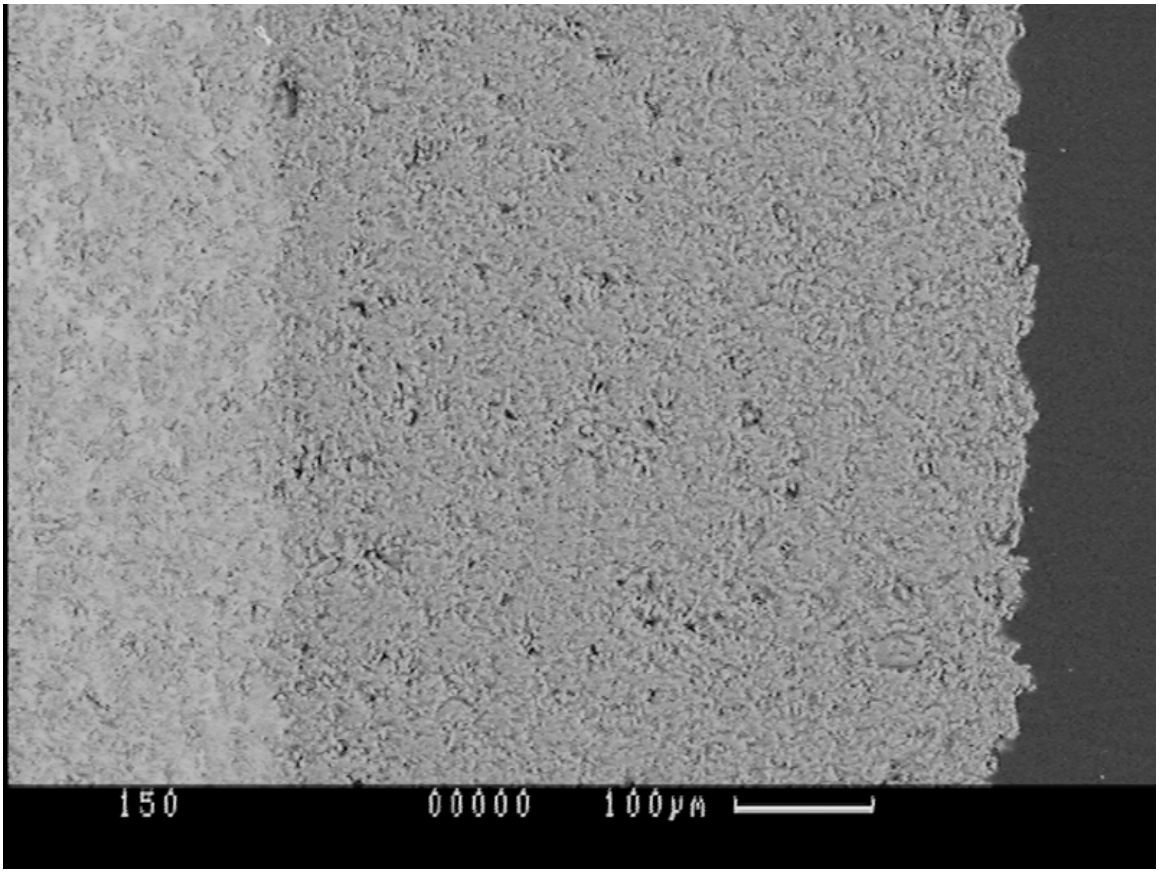

Figure 5.4. Lot 1-1A Cross-section 150X.

Figure 5.5 shows the microscopic structure of the plasma sprayed alumina. This picture as well as Figure 5.4 show voids in the alumina coating. The porosity of the coating allows air and moisture to be present within the coating and leads to a lower dielectric breakdown voltage. Moisture, from the humidity in the air, becomes trapped within the voids and results in a lower dielectric strength. As shown in Figure 5.1, coupon 1A is tested without the trapped moisture being removed and has a dielectric strength of 4560 V while Coupons 2A and 3A each have a dielectric strength above 5500 V.

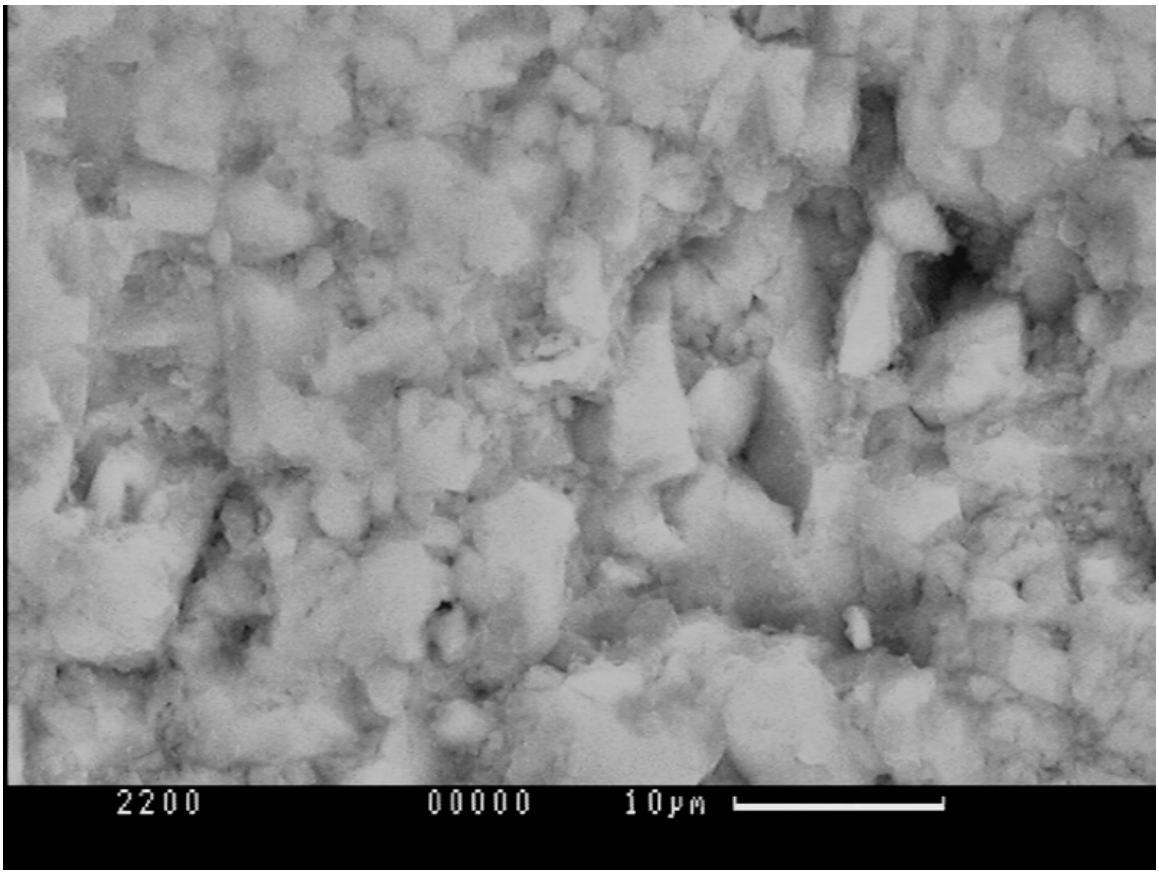

Figure 5.5. Lot 1-1A Plasma Spray Alumina Microstructure 2200X.

Figure 5.6 illustrates the elemental analysis of the plasma spray alumina coating. The figure shows that aluminum is the only element present. Oxygen cannot be determined by this test and therefore is not shown in the picture. Figure 5.7 shows the elemental analysis of the AlSiC MMC baseplate. Only the aluminum and silicon are shown in the data since carbon is another element not determined with this test.

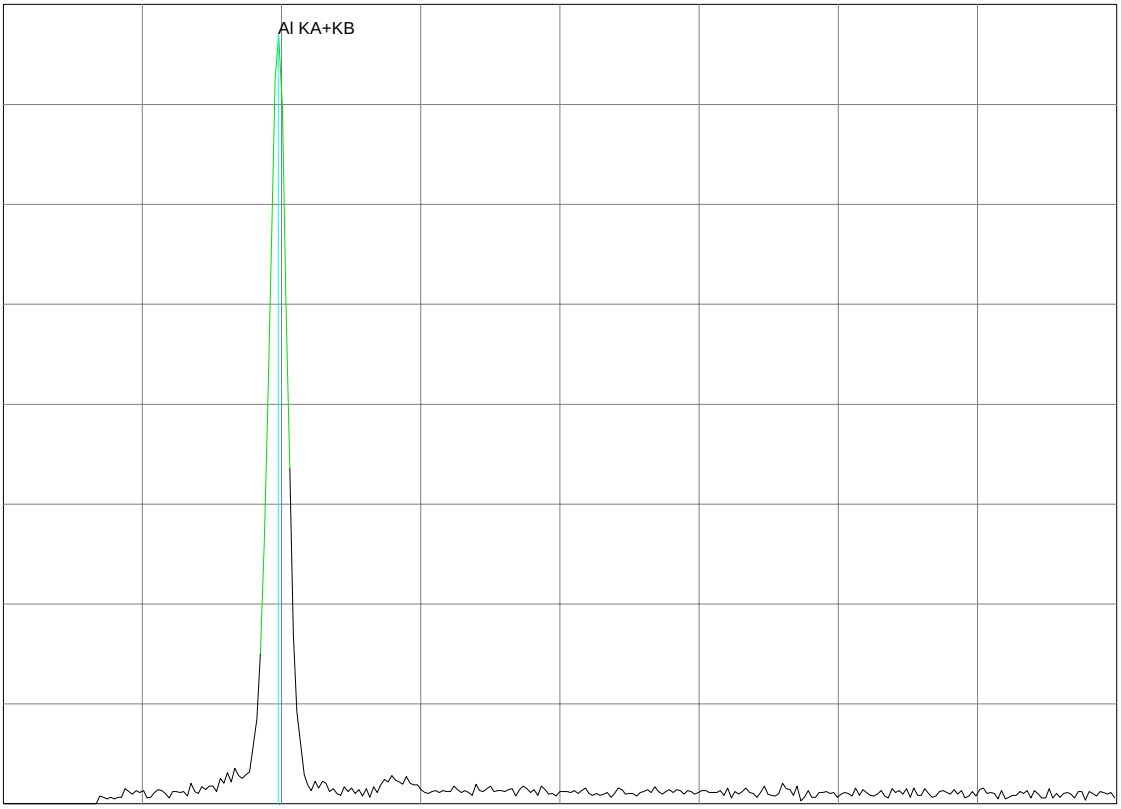

Figure 5.6. Lot 1-1A Plasma Spray Alumina Elemental Analysis.

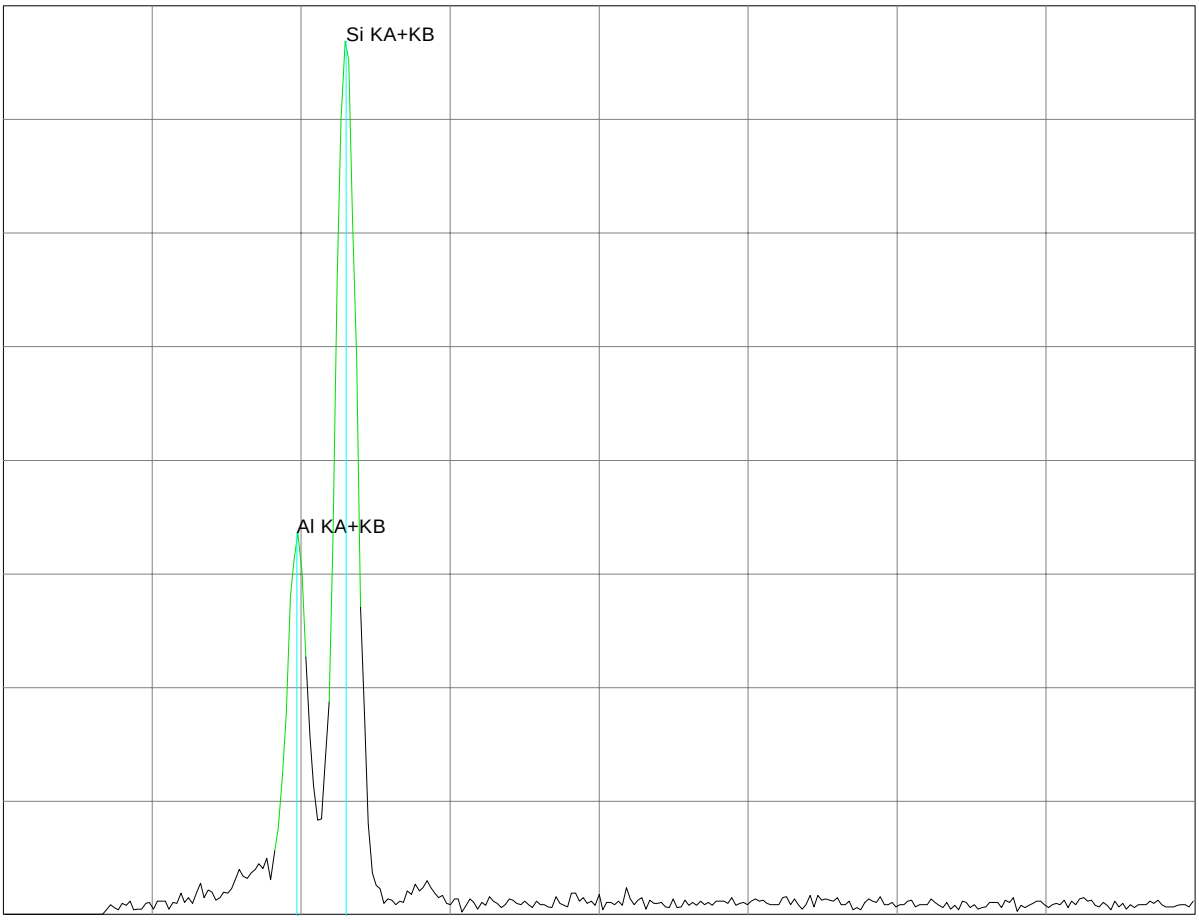

Figure 5.7. Lot 1-1A AlSiC MMC Elemental Analysis.

5.3 Lot 2 Plasma Spray Alumina 5000 V

Lot 2 consists of four coupons manufactured using plasma spray technology and rated to have a minimum dielectric strength of 5000 V. The thickness of the alumina isolation layer is measured to be 30 - 33 mils. Figure 5.8 shows a graphical presentation of direct-voltage dielectric breakdown voltages tests performed on Lot 2 Coupons 1A, 2A, and 3A. Coupon 1A is tested "as shipped" from the manufacturer, Coupon 2A is tested after being conditioned for 24 hours at 125 ºC, and Coupon 3A is tested after being conditioned for 24 hours at 200 ºC. All coupons tested exceed the manufacturers rating concerning dielectric breakdown voltage.

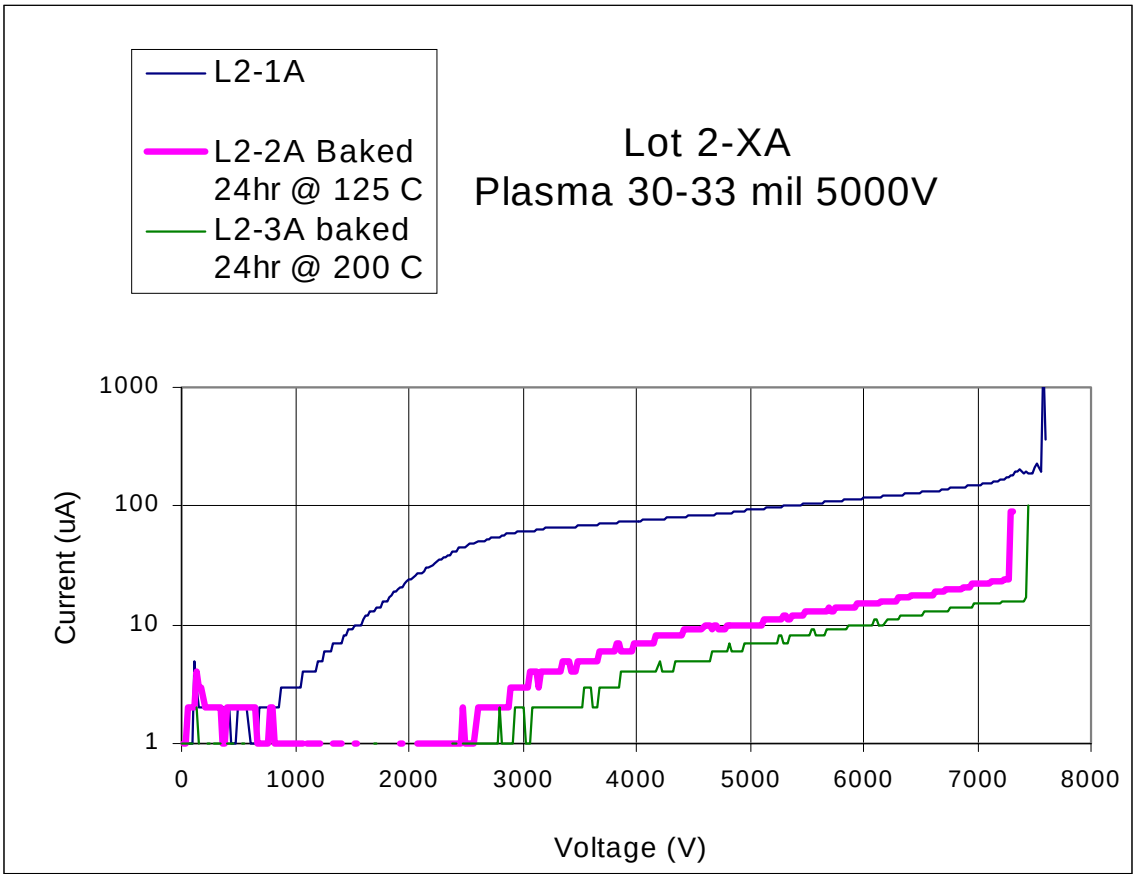

Figure 5.8. Dielectric Breakdown Voltage Results Lot 2-xA.

Figure 5.9 illustrates the results of a direct-voltage leakage current test perform on coupon 4A with three different scenarios. Coupon 4A is tested as shipped, conditioned 24 hours at 125 ºC, and then conditioned for an additional 24 hours at 200 ºC. Figure 5.9 shows that when the coupon is tested "as shipped", the leakage current is higher and most likely due to trapped moisture. Conditioning at 125 ºC removed the trapped moisture and additional conditioning at 200 ºC gave no improvements.

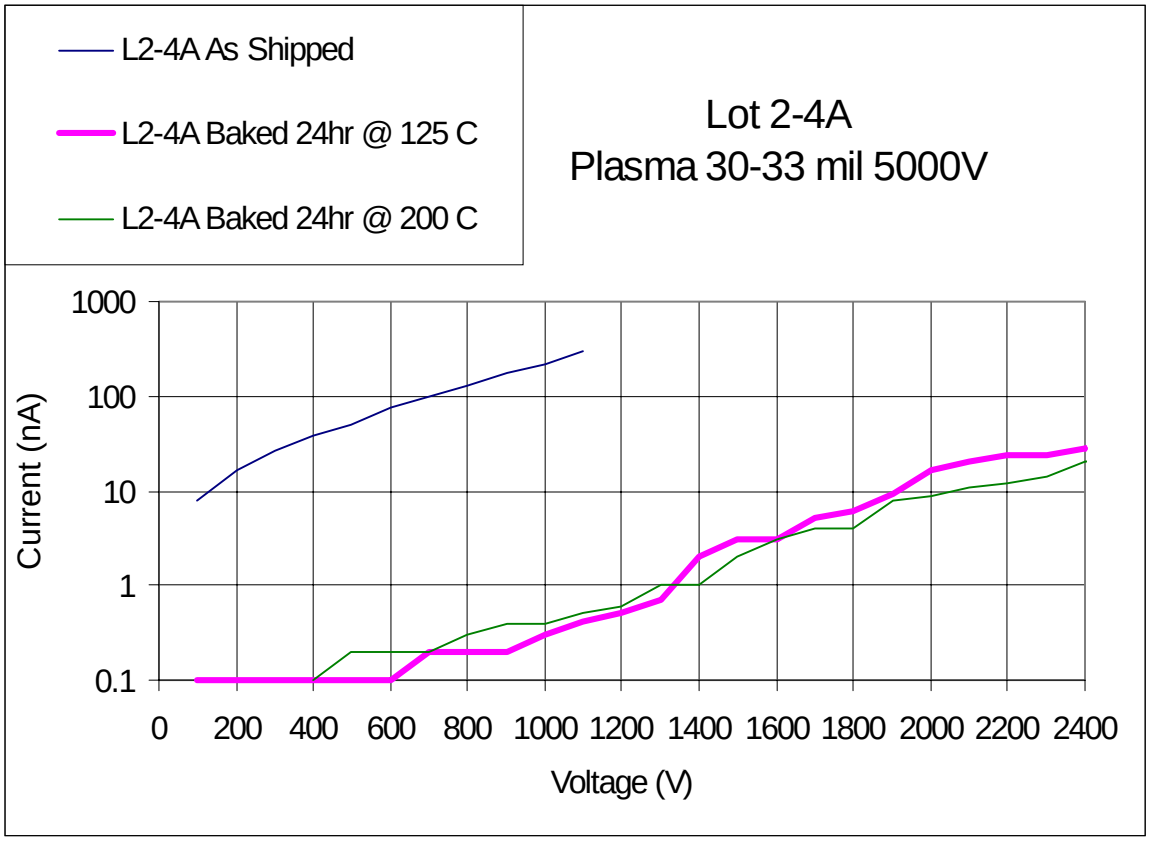

Figure 5.9. Lot 2-4A Dielectric Leakage Current Test.

Figure 5.10 shows a graphical presentation of direct-voltage dielectric breakdown voltages tests performed on Lot 2 Coupons 1B, 2B, and 3B. Coupon 1B is tested as shipped from the manufacture, Coupon 2B is tested after being conditioned for 24 hours at 125 ºC, and Coupon 3B is tested after being conditioned for 24 hours at 200 ºC.

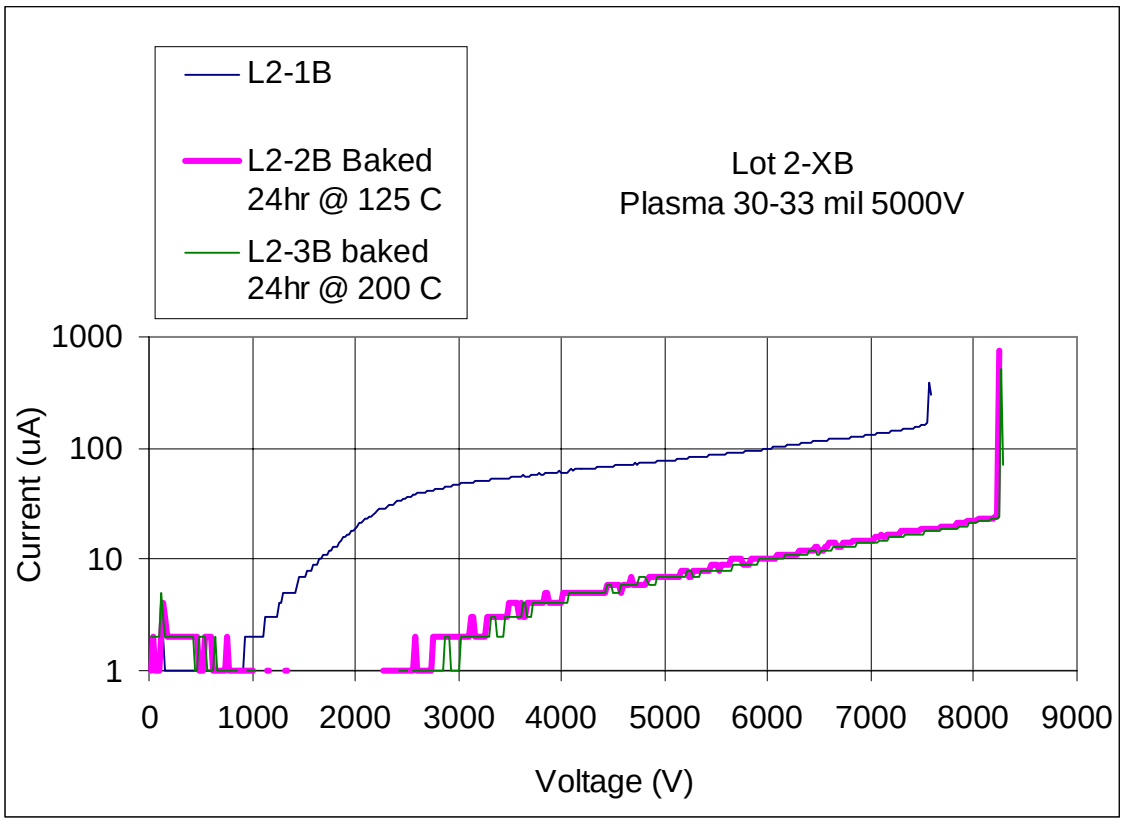

Figure 5.10. Dielectric Breakdown Voltage Results Lot 2-xB.

The interface between the AlSiC MMC baseplate and the alumina ceramic insulative layer is shown in Figure 5.11. The picture is the cross-section of Lot 2-1A using a SEM with backed scanned electron enhancement. The lack of voids and cracks, not seen in the cross-sectional view, implies excellent adhesion and good mechanical bonding. The interface between the AlSiC MMC baseplate and the alumina ceramic insulative layer must have a maximum percent of surface contact to insure the maximum amount of heat can be transferred across the interface. The picture also illustrates the surface roughness of the plasma sprayed alumina. This can lead to problems in bonding a layer of metallization to the alumina.

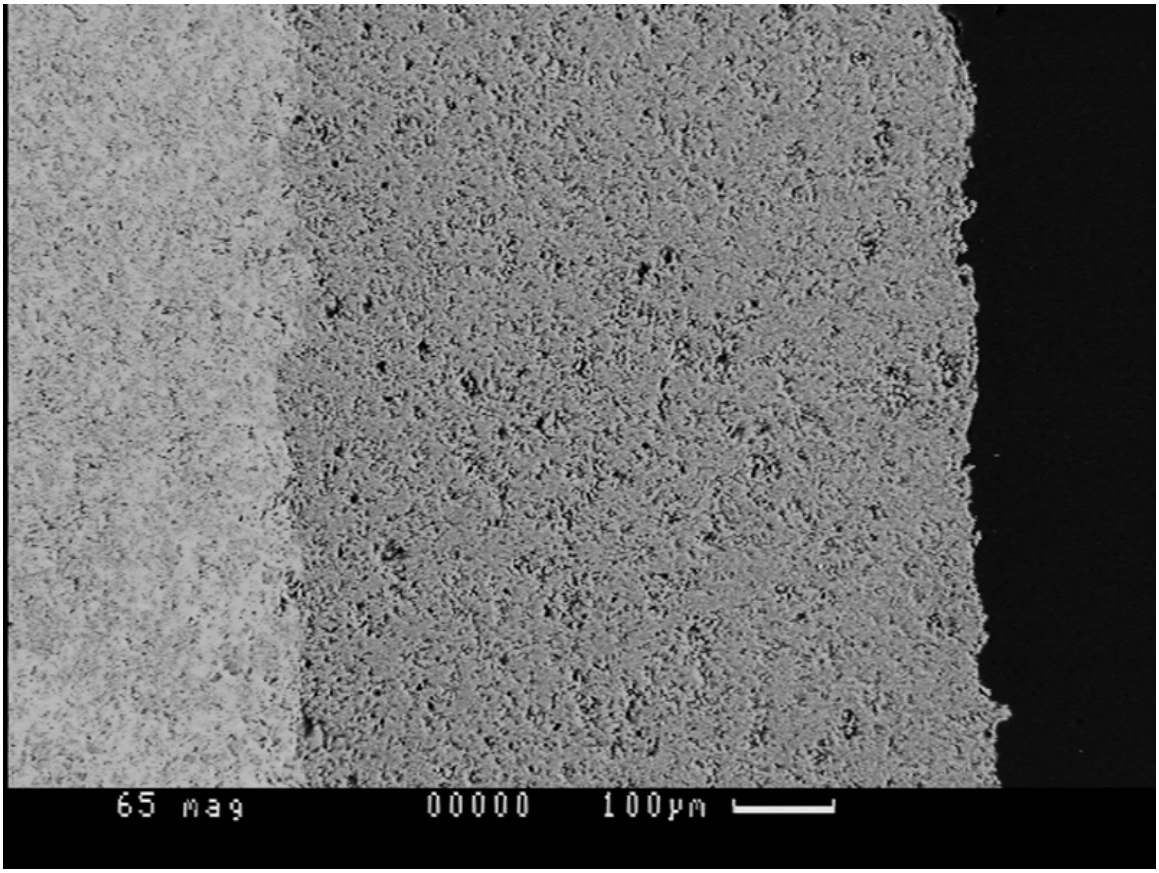

Figure 5.11. Lot 2-1A Cross-section 65X.

Figure 5.12 shows the microscopic structure of the plasma sprayed alumina. This picture as well as Figure 5.11, show voids in the alumina coating. The porosity of the coating allows air and moisture to be present within the coating and leads to a lower dielectric breakdown voltage. The porosity resulting from plasma spray coatings can be in the range of 5 to 30%.[6]

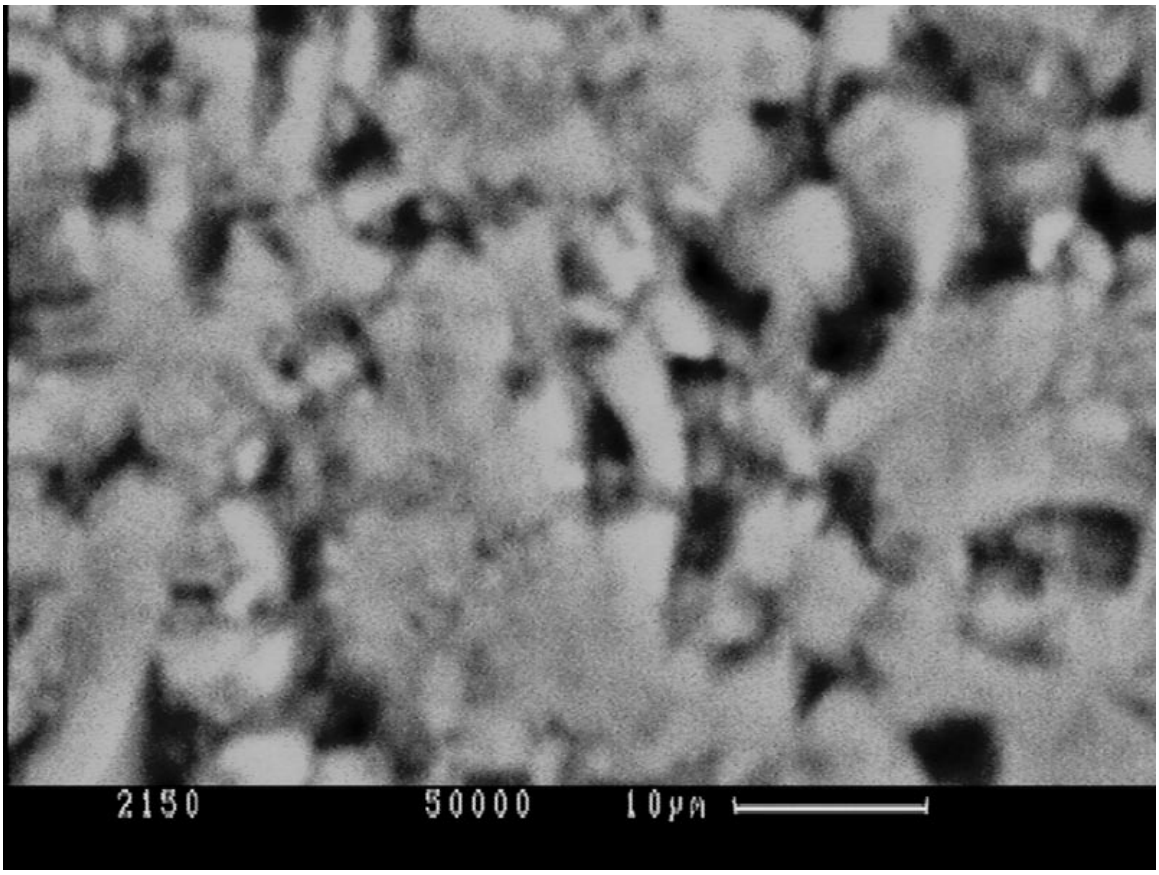

Figure 5.12. Lot 2-1A Plasma Spray Alumina Microstructure 2150X.

Figure 5.13 shows that actual dielectric breakdown path of Coupon Lot 2-1A. In preparing a cross-sectional slice of the test coupon, the saw sliced through the breakdown path giving an excellent illustration of the path taken. When viewed under a microscope, the path looks like a worm hole from the surface of the alumina to the AlSiC MMC. Notice the crater at the surface of the alumina.

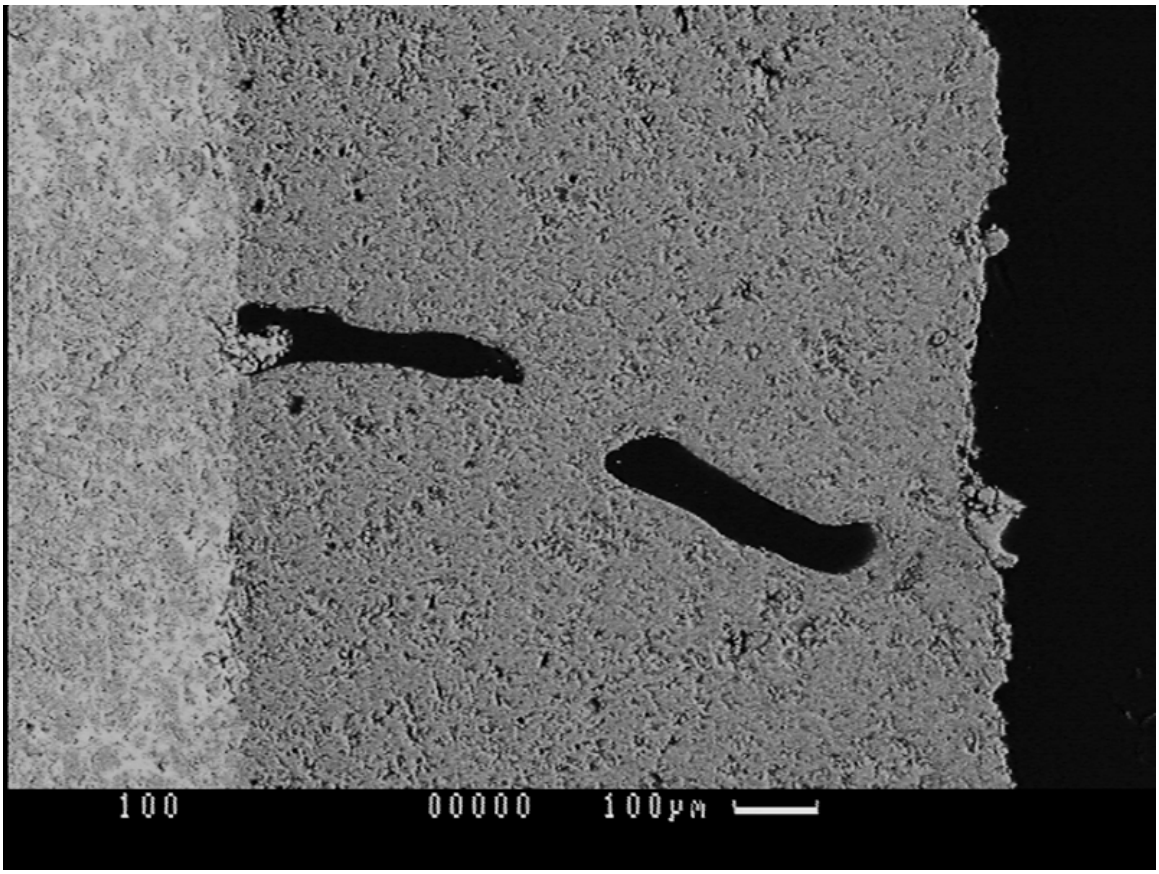

Figure 5.13. Lot 2-1A Dielectric Breakdown Path 100X.

Figure 5.14 illustrates the elemental analysis of the plasma spray alumina coating. Only the aluminum is shown in the data since oxygen can not be determined by this test. Figure 5.15 shows the elemental analysis of the AlSiC MMC baseplate. Only the aluminum and silicon are shown in the data since carbon can not be determined by this test. Figure 5.14 shows a small amount of silicon present.

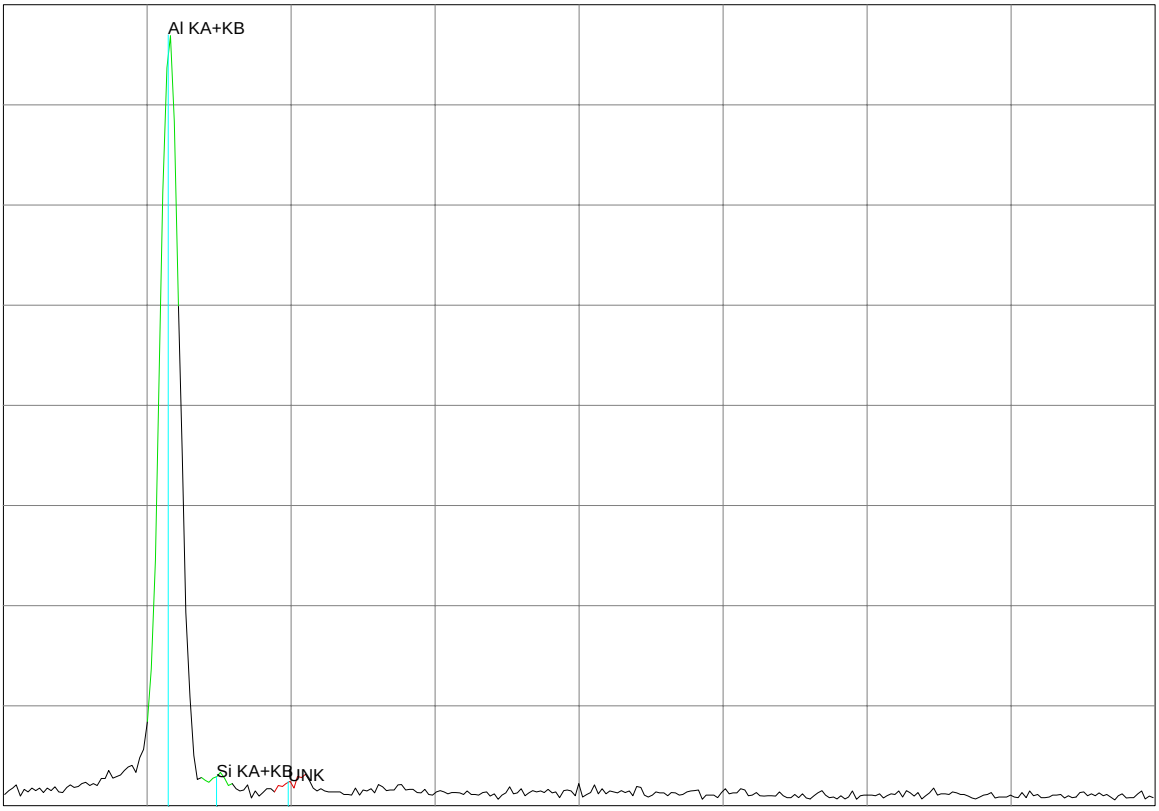

Figure 5.14. Lot 2-1A Plasma Spray Alumina Elemental Analysis.

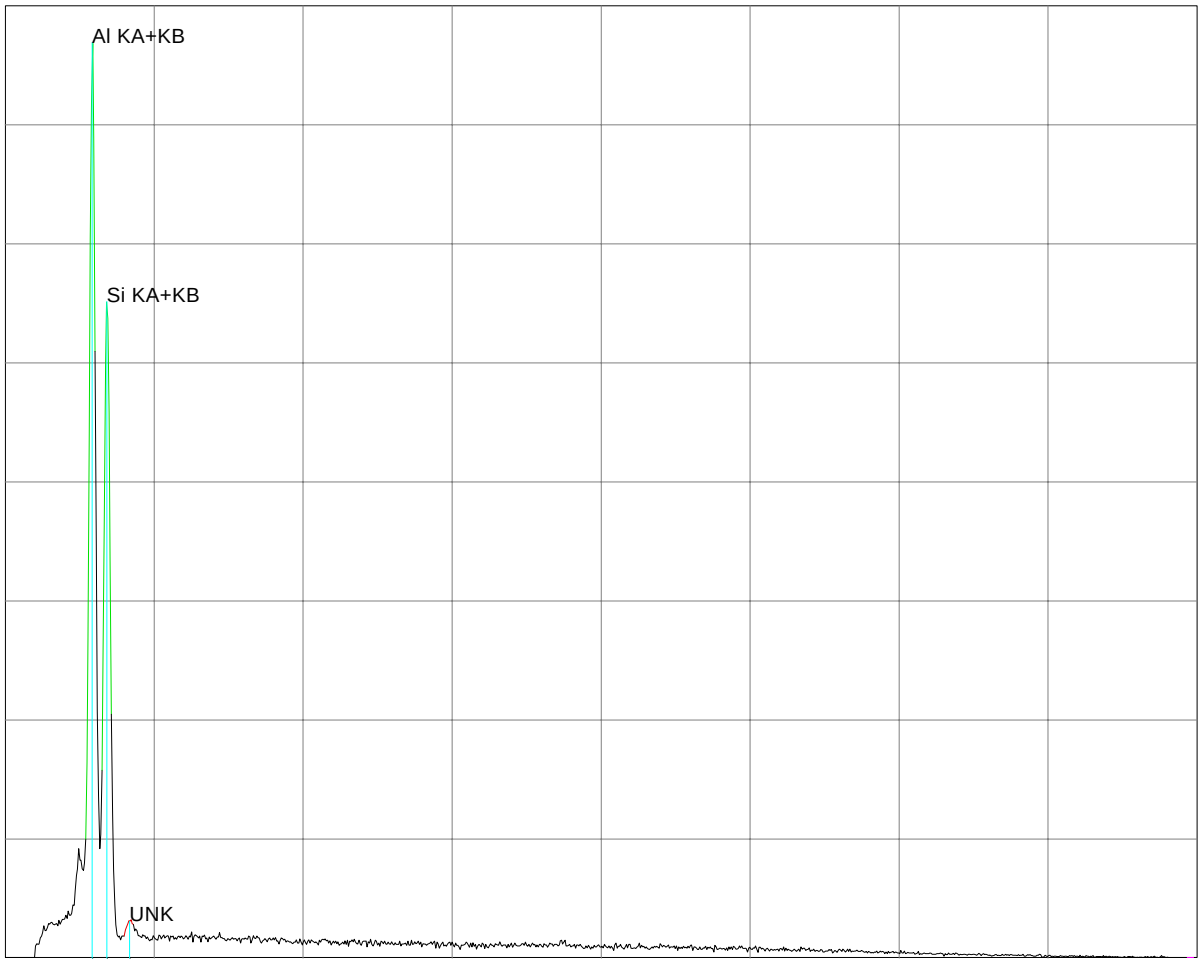

Figure 5.15. Lot 2-1A AlSiC MMC Elemental Analysis.

5.4 Lot 3 High Velocity Oxyfuel Spray Alumina 3000 V

Lot 3 consists of four coupons manufactured using HVOF spray technology and rated to have a minimum dielectric strength of 3000 V. The thickness of the alumina isolation layer is measured to be 6 - 7 mils. Figure 5.16 shows a graphical presentation of direct-voltage dielectric breakdown voltages tests performed on Lot 3 Coupons 1A, 2A, and 3A. Coupon 1A is tested as shipped from the manufacture, Coupon 2A is tested after being conditioned for 24 hours at 125 ºC, and Coupon 3A is tested after being conditioned for 24 hours at 200 ºC. All coupons exceed their dielectric strength rating and conditioning affected both the breakdown voltage and leakage current.

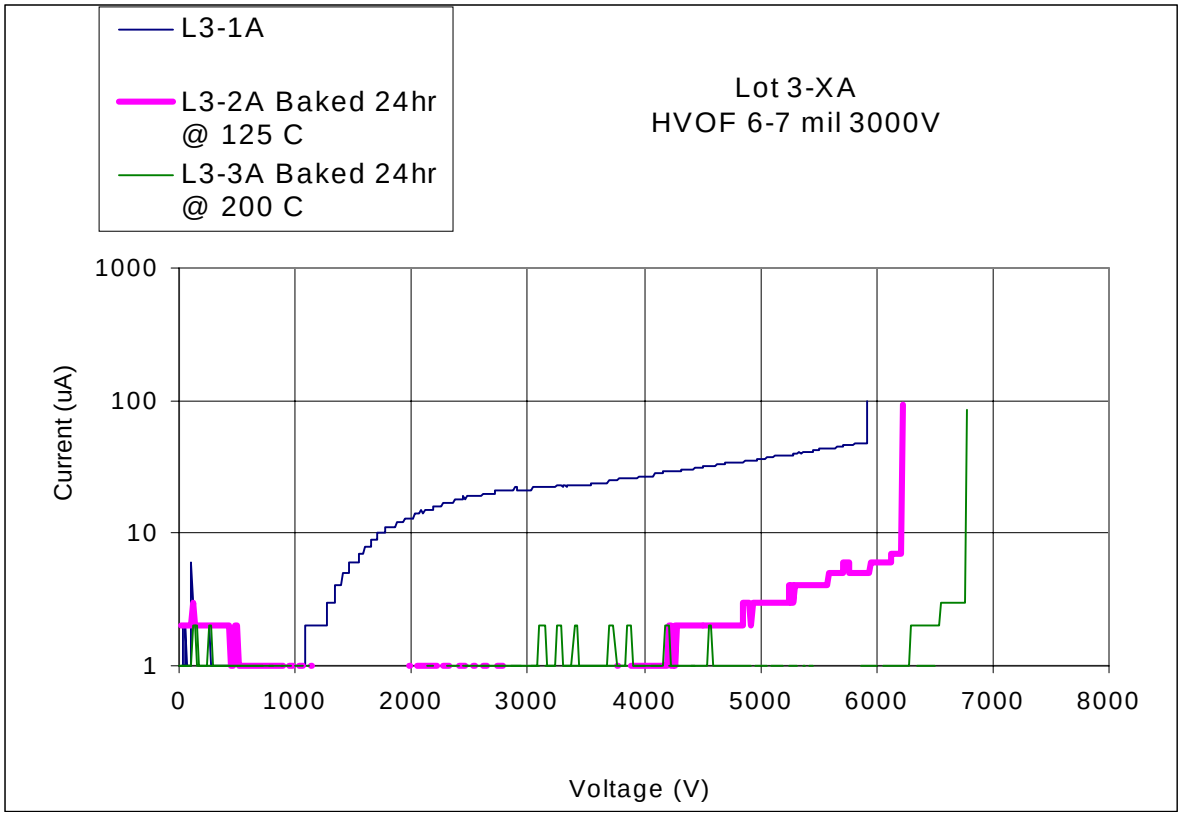

Figure 5.16. Dielectric Breakdown Voltage Results Lot 3-xA.

Figure 5.17 shows the results of a direct-voltage leakage current test perform on coupon 4A with three different scenarios. Coupon 4A is tested as shipped, conditioned 24 hours at 125 ºC, and then conditioned for an additional 24 hours at 200 ºC. Trapped moisture seems to be present when tested "as shipped" and is removed when conditioned at 125 ºC. Little improvement is obtained by additional conditioning at 200 ºC. Testing could not be done for all voltages due to current spikes at the high voltages making the data impossible to record. Conditioned samples had steady leakage currents up to normal maximum operating voltages of 1500 – 1600 V.

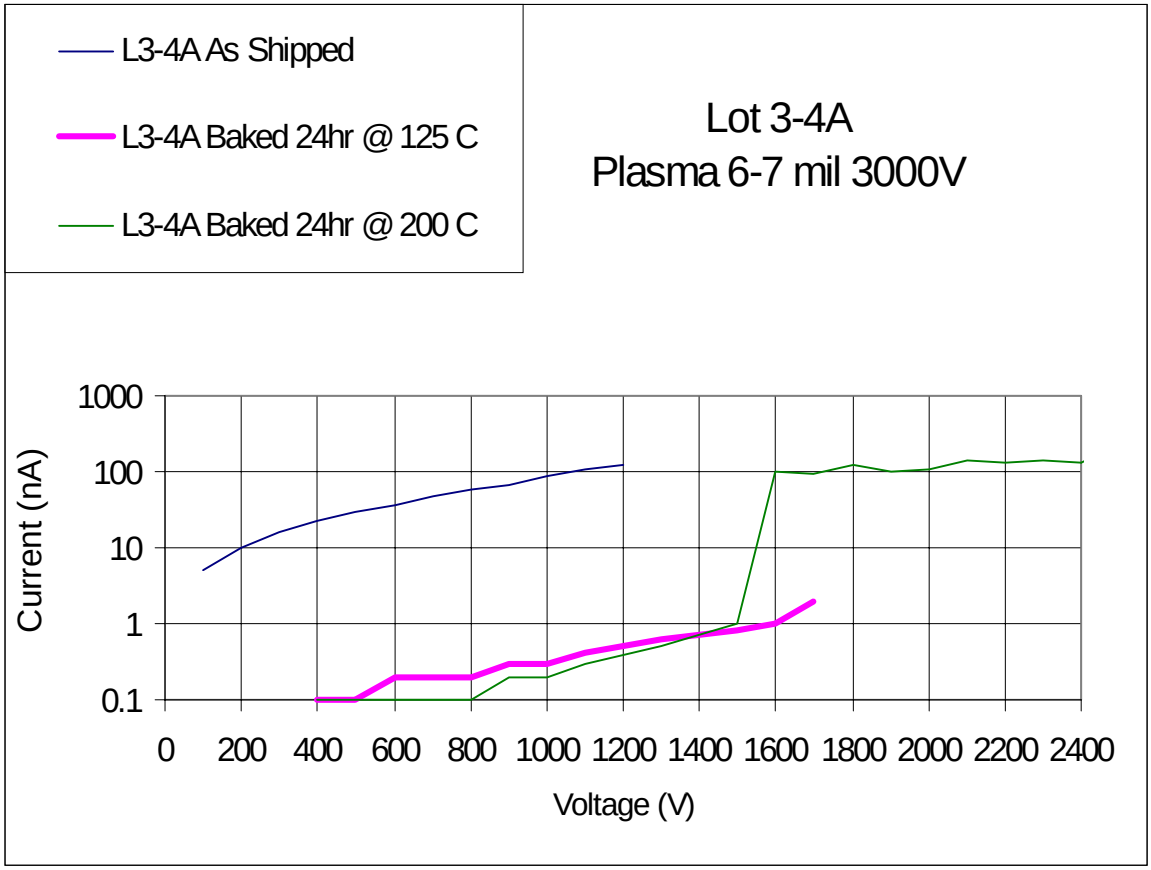

Figure 5.17. Lot 3-4A Dielectric Leakage Current Test.

Figure 5.18 illustrates a graphical presentation of direct-voltage dielectric breakdown voltages tests performed on Lot 1 Coupons 1B, 2B, and 3B. Coupon 1B is tested as shipped from the manufacture, Coupon 2B is tested after being conditioned for 24 hours at 125 ºC, and Coupon 3B is tested after being conditioned for 24 hours at 200 ºC. Figure 5.18 shows that all coupons exceeded their dielectric breakdown voltage rating. Moisture seems to be present in 1B lowering dielectric strength and raising the leakage current.

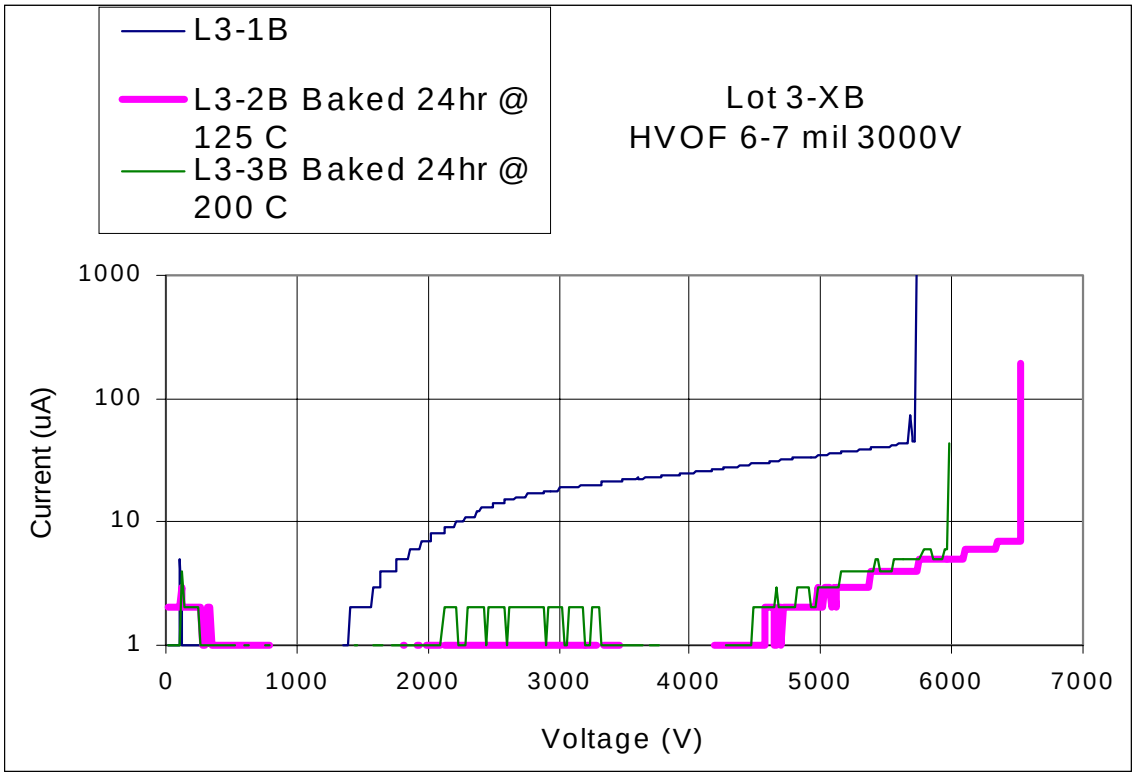

Figure 5.18. Dielectric Breakdown Voltage Results Lot 3-xB.

The interface between the AlSiC MMC baseplate and the alumina ceramic insulative layer is shown in Figure 5.19. The picture is the cross-section of Lot 3-1A using a SEM with backed scanned electron enhancement. As HVOF sprayed alumina particles impinge the surface of the substrate, they conform to the substrate surface creating a mechanical bond. The lack of voids and cracks, not seen in the cross-sectional view, implies excellent adhesion and good mechanical bonding. The picture also illustrates the surface roughness of the HVOF sprayed alumina. This can lead to problems in bonding a layer of metallization to the alumina.

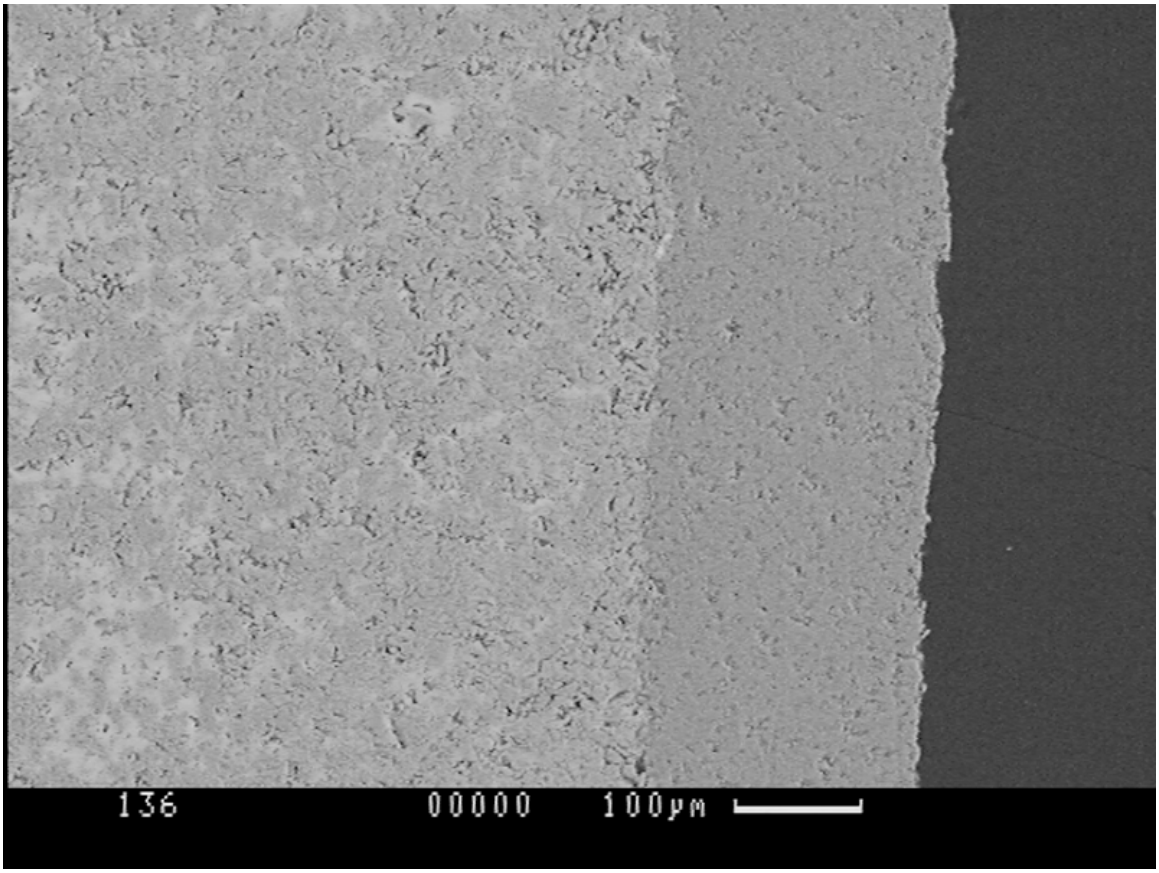

Figure 5.19. Lot 3-1A Cross-section 136X.

Figure 5.20 shows the microscopic structure of the HVOF sprayed alumina. This picture as well as Figure 5.19 shows voids in the alumina coating. The porosity of the coating allows air and moisture to be present within the coating and leads to a lower dielectric breakdown voltage. The porosity resulting from HVOF spray coatings is normally lower than with plasma spray coating translating into a denser coating. A comparison between Figure 5.20 and Figure 5.12 illustrates the difference in materials' densities.

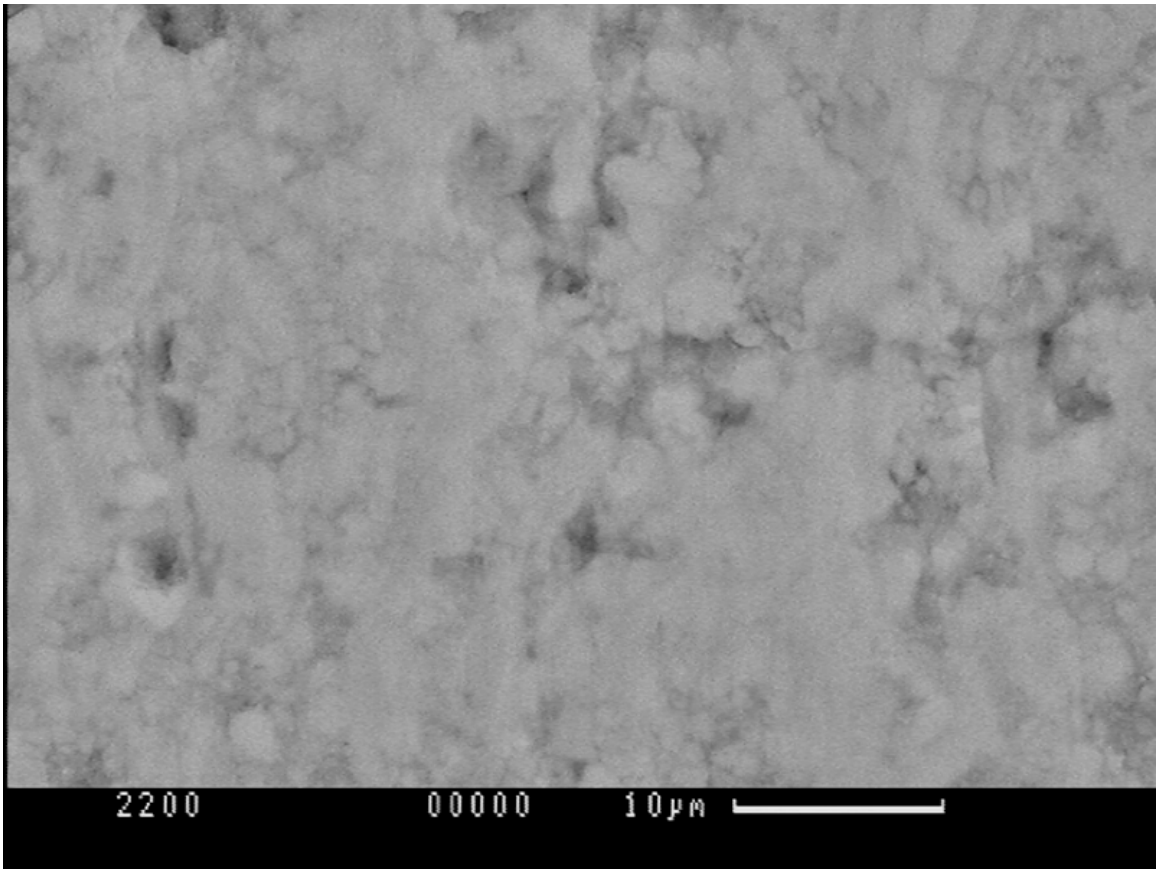

Figure 5.20. Lot 3-1A HVOF Spray Alumina Microstructure 2200X.

Figure 5.21 shows the elemental analysis of the HVOF spray alumina coating. Only the aluminum is shown in the data since oxygen can not be determined by this test. The purity of the coating is illustrated in Figure 5.21. Figure 5.22 shows the elemental analysis of the AlSiC MMC baseplate. Only the aluminum and silicon are shown in the data since carbon can not be determined by this test. The purity of the coating and the proportionality of the elements are illustrated in Figure 5.22.

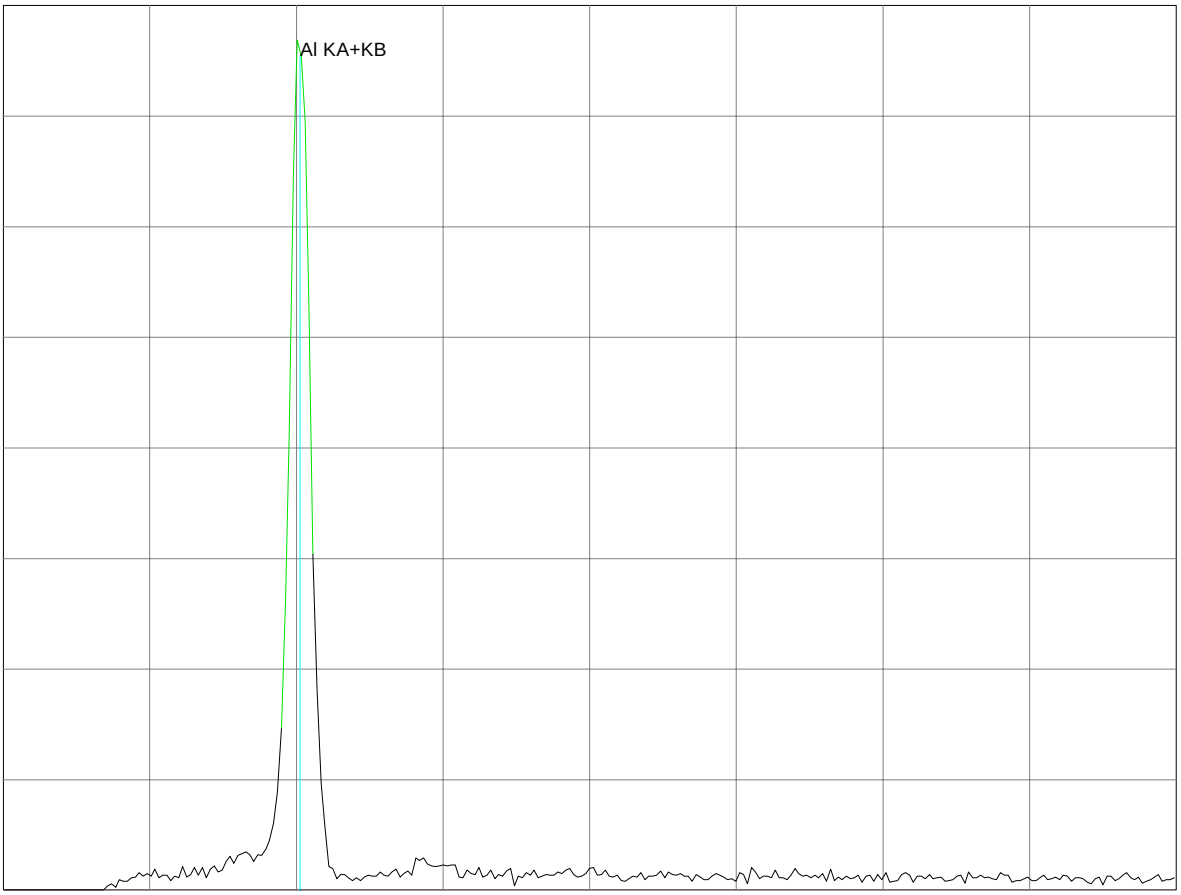

Figure 5.21. Lot 3-1A HVOF Spray Alumina Elemental Analysis.

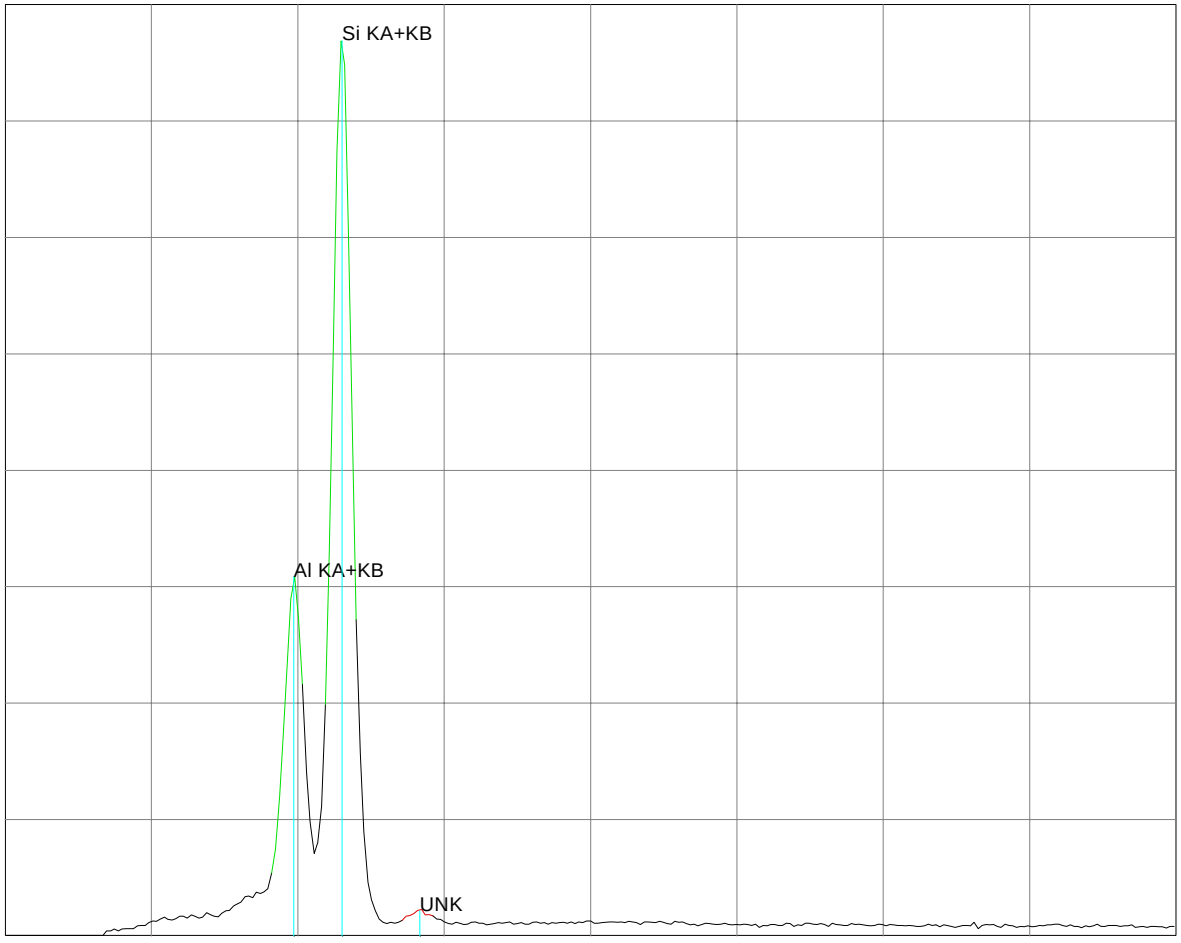

Figure 5.22. Lot 3-1A AlSiC MMC Elemental Analysis.

5.5 Lot 4 HVOF Spray Alumina 5000 V

Lot 4 consists of four coupons manufactured using HVOF spray technology and rated to have a minimum dielectric strength of 5000 V. The thickness of the alumina isolation layer is measured to be 13 - 14 mils. Figure 5.23 shows a graphical presentation of direct-voltage dielectric breakdown voltages tests performed on Lot 1 Coupons 1A, 2A, and 3A. Coupon 1A is tested as shipped from the manufacture, Coupon 2A is tested after being conditioned for 24 hours at 125 ºC, and Coupon 3A is tested after being conditioned for 24 hours at 200 ºC. All coupons exceed their dielectric strength rating and conditioning affected both the breakdown voltage and the leakage current.

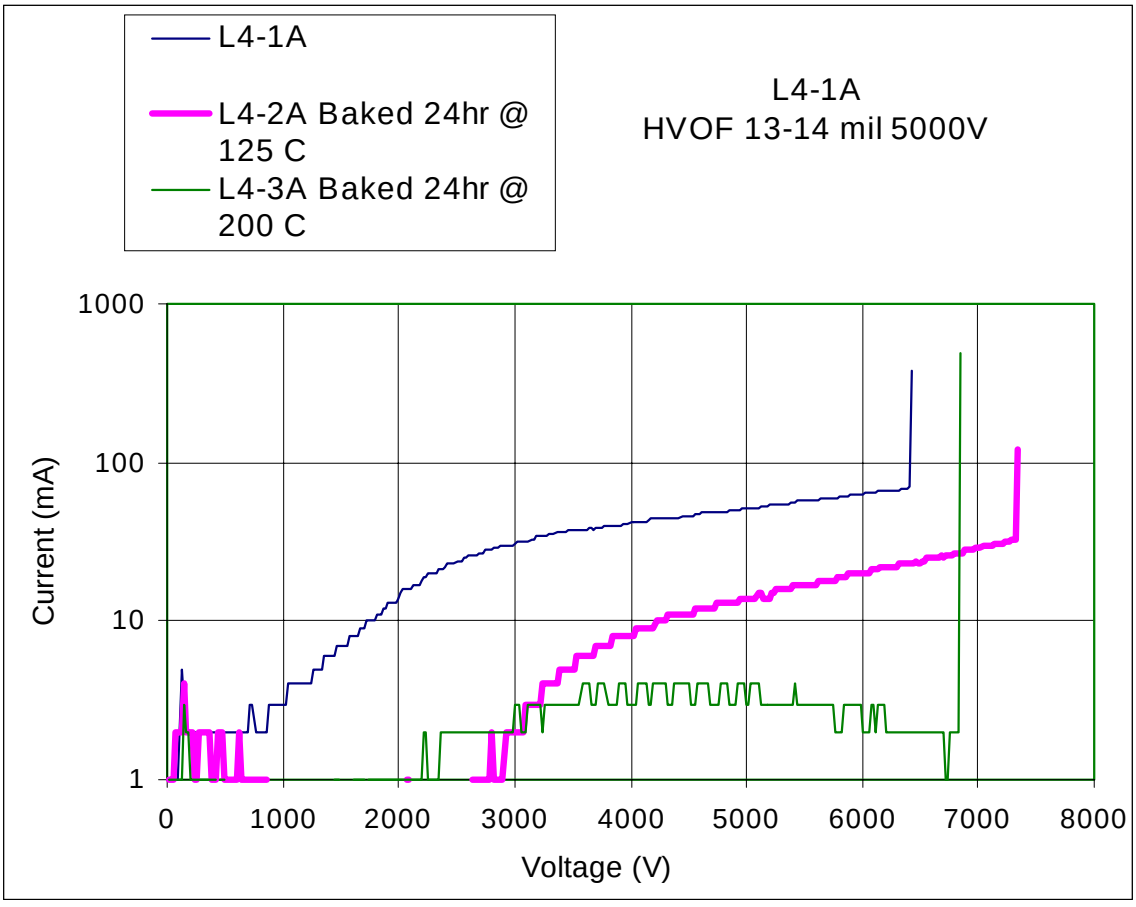

Figure 5.23. Dielectric Breakdown Voltage Results Lot 4-xA.

Figure 5.24 shows the results of a direct-voltage leakage current test perform on coupon 5A with three different scenarios. Coupon 5A is tested as shipped, conditioned 24 hours at 125 ºC, and then conditioned for an additional 24 hours at 200 ºC. Trapped moisture seems to be present when tested "as shipped" and is removed when conditioned at 125 ºC. Little improvement is obtained by additional conditioning at 200 ºC. Testing could not be done for all voltages due to current spikes at the high voltages making the data impossible to record. Conditioned samples had steady leakage currents up to normal maximum operating voltages of 1400 – 1600 V.

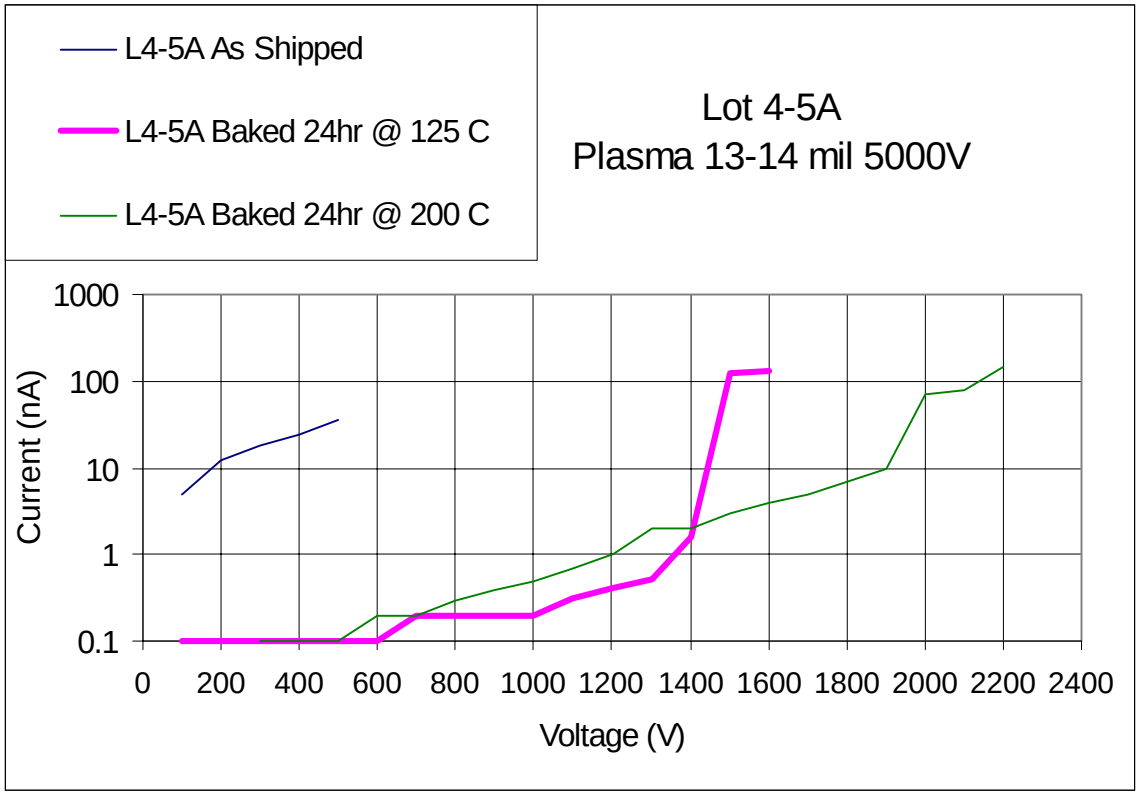

Figure 5.24. Lot 4-5A Dielectric Leakage Current Test.

Figure 5.25 shows a graphical presentation of direct-voltage dielectric breakdown voltages tests performed on Lot 4 Coupons 1B, 2B, and 3B. Coupon 1B is tested as shipped from the manufacture, coupon 2B is tested after being conditioned for 24 hours at 125 ºC, and Coupon 3B is tested after being conditioned for 24 hours at 200 ºC. Figure 5.25 shows that all coupons exceeded their dielectric breakdown voltage rating.

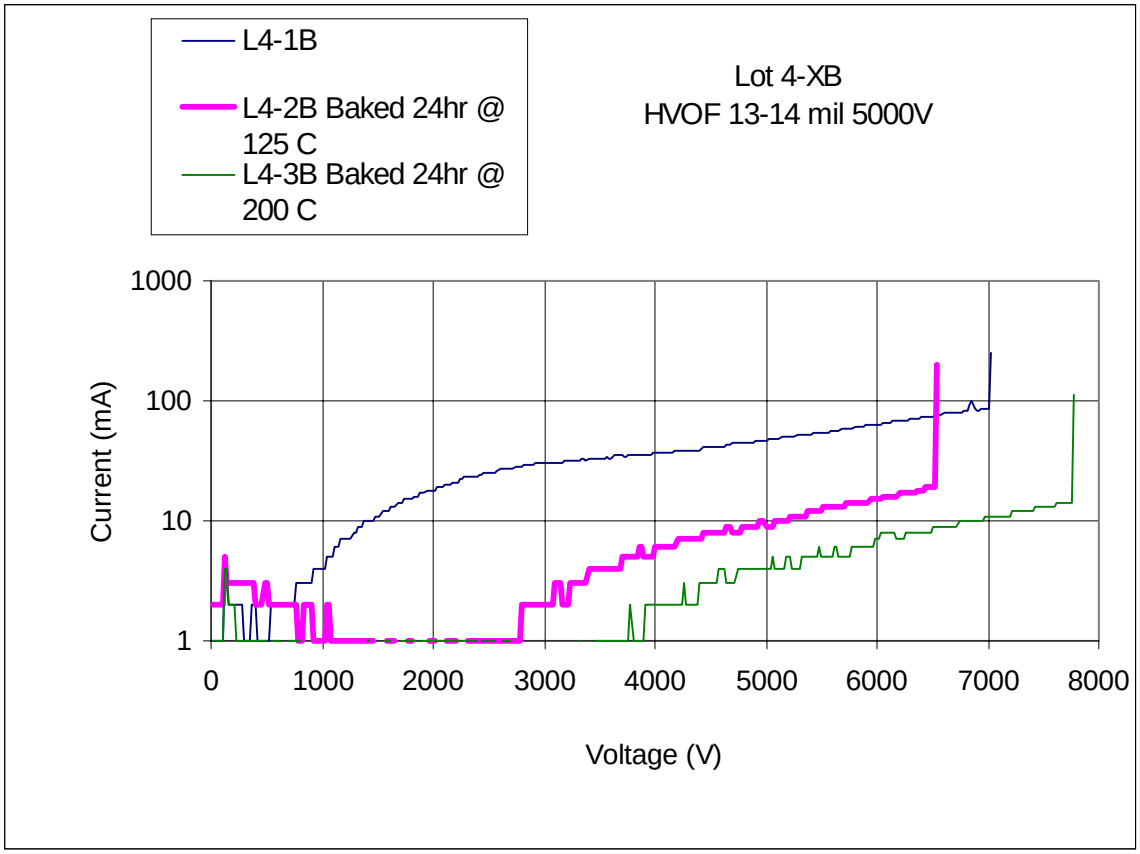

Figure 5.25. Dielectric Breakdown Voltage Results Lot 4-xB.

The interface between the AlSiC MMC baseplate and the alumina ceramic insulative layer is shown in Figure 5.26. The picture is the cross-section of Lot 4-1A using a SEM with backed scanned electron enhancement. As HVOF sprayed alumina particles impinge the surface of the substrate, they conform to the substrate surface creating a mechanical bond. The lack of voids and cracks, not seen in the cross-sectional view, implies excellent adhesion and good mechanical bonding. The picture also illustrates the surface roughness of the HVOF sprayed alumina. This can lead to problems in bonding a layer of metallization to the alumina.

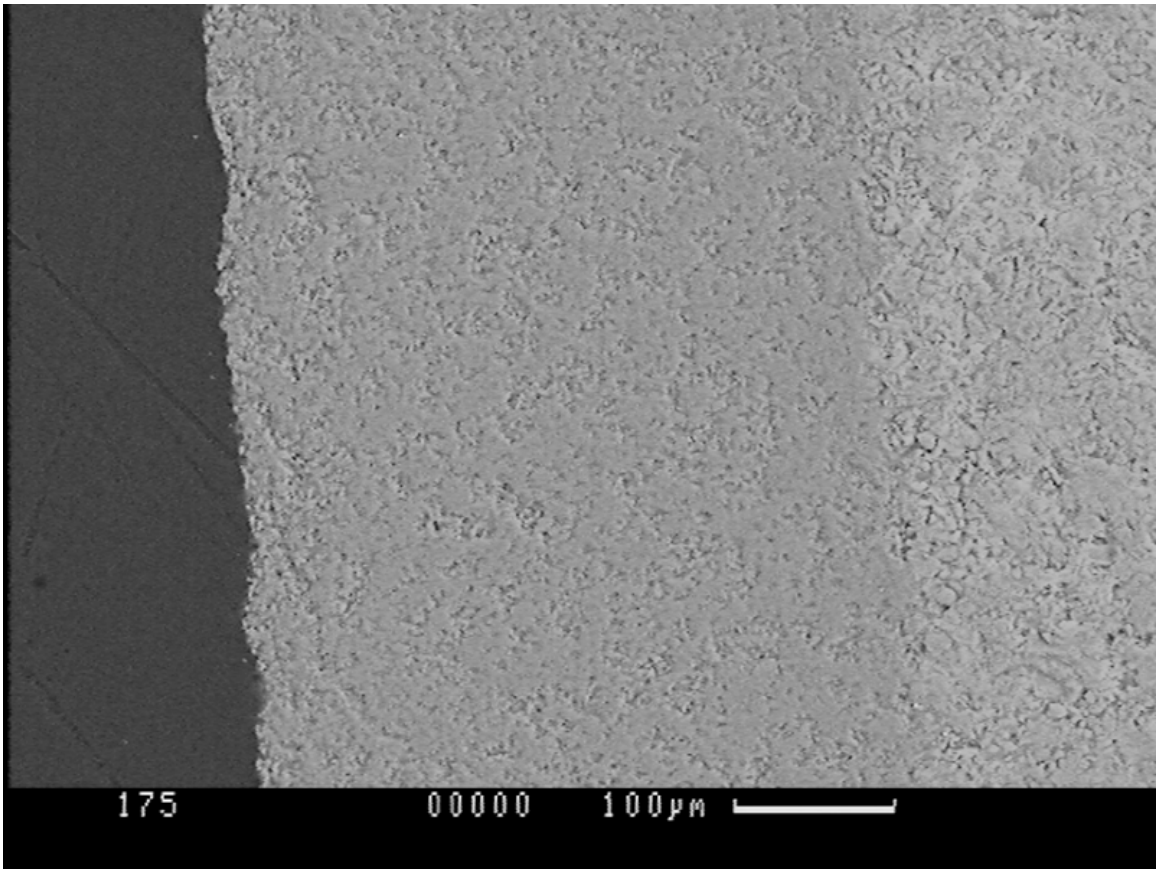

Figure 5.26. Lot 4-1A Cross-section 175X.

Figure 5.27 shows the microscopic structure of the HVOF sprayed alumina. This picture as well as figure 5.26 show voids in the alumina coating. The porosity of the coating allows air and moisture to be present within the coating and leads to a lower dielectric breakdown voltage. The porosity resulting from HVOF spray coatings is normally lower than with plasma spray coating translating into a denser coating.

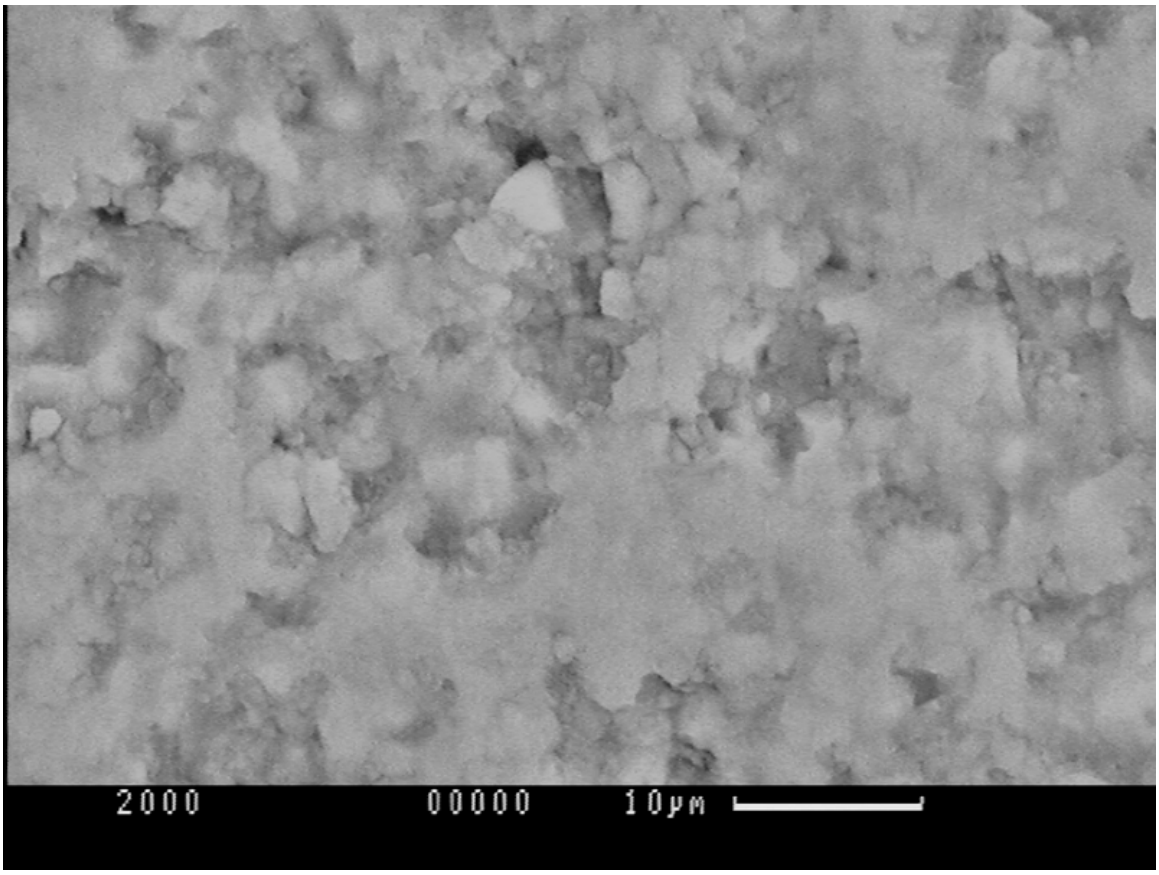

Figure 5.27. Lot 4-1A HVOF Spray Alumina Microstructure 2000X.

Figure 5.28 shows the elemental analysis of the HVOF spray alumina coating. Only the aluminum is shown in the data since oxygen can not be determined by this test. The purity of the coating is illustrated in Figure 5.28. Figure 5.29 shows the elemental analysis of the AlSiC MMC baseplate. Only the aluminum and silicon are shown in the data since carbon can not be determined by this test. The purity of the coating and the proportionality of the elements are illustrated in Figure 5.29.

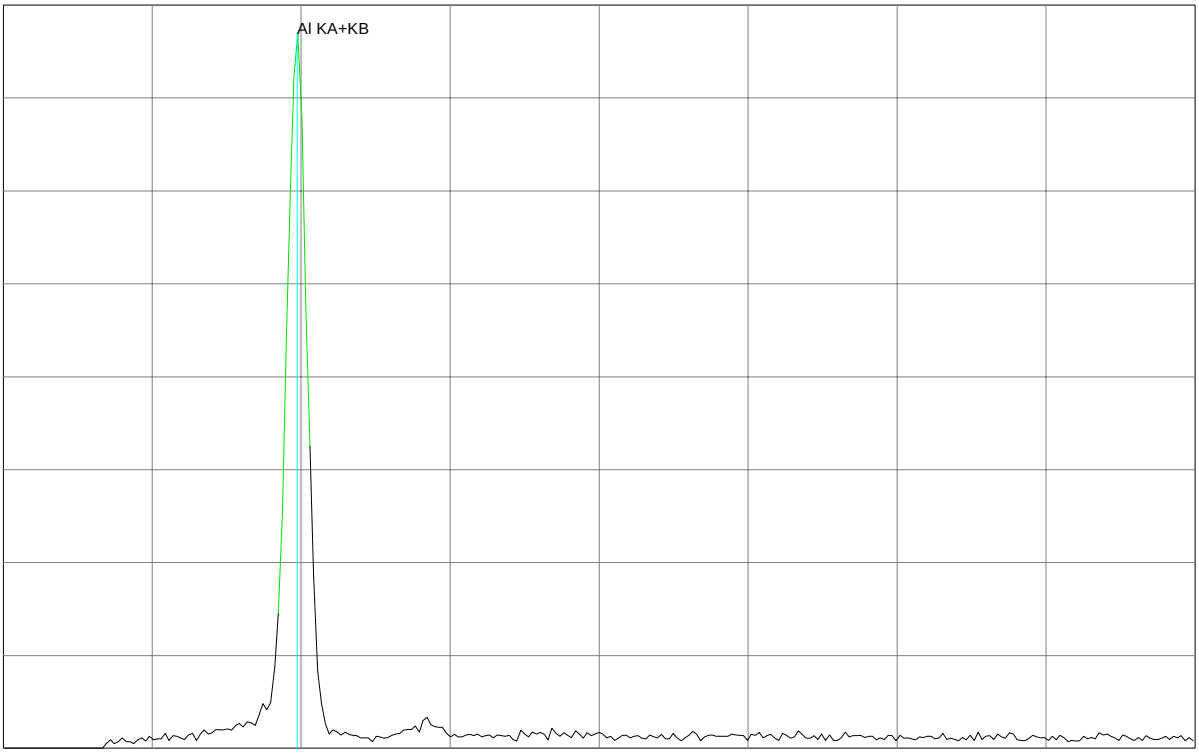

Figure 5.28. Lot 4-1A HVOF Spray Alumina Elemental Analysis.

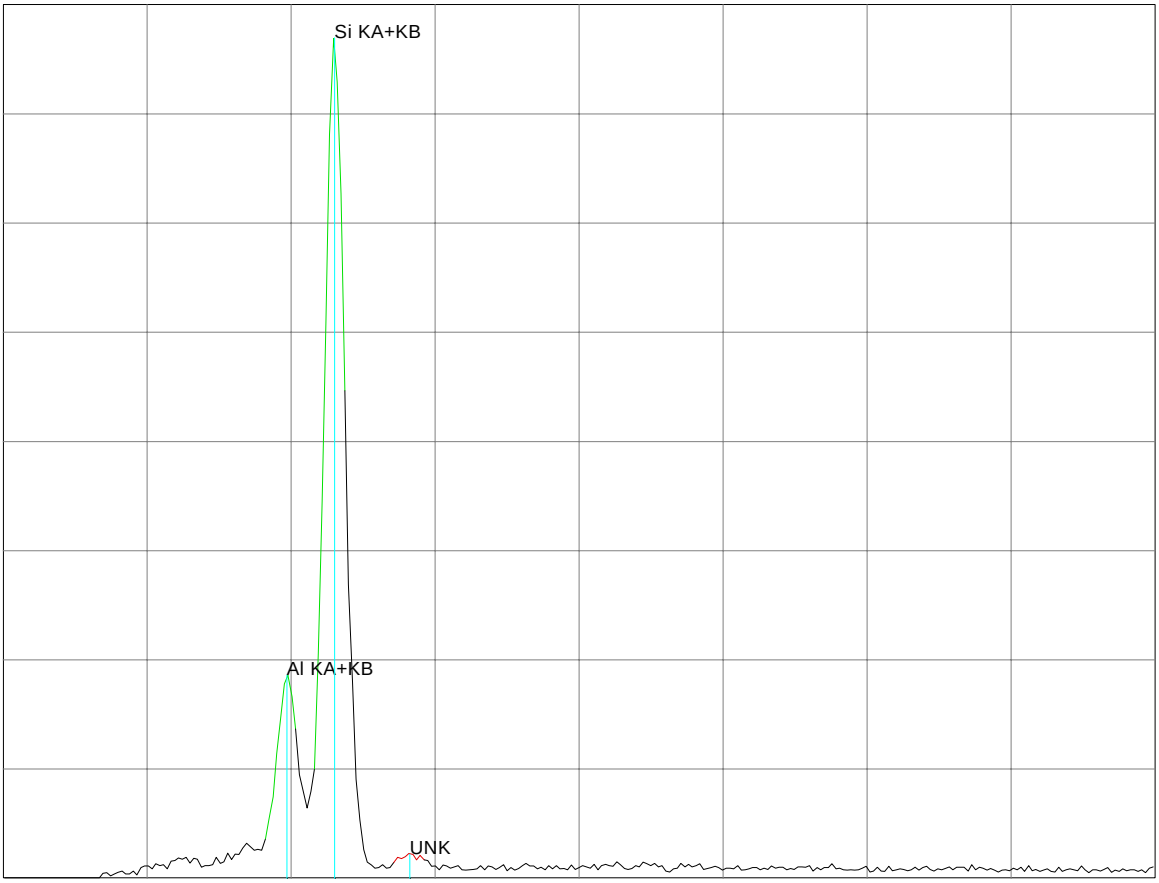

Figure 5.29. Lot 4-1A AlSiC MMC Elemental Analysis.

5.6 Lot 5 Alumina Substrate 25 mil Thick

Lot 5 consists of an alumina substrate with is 25 mil thick. Figure 5.30 shows a graphical presentation of direct-voltage dielectric breakdown voltages tests performed on Lot 5. Dielectric breakdown occurred at 16.4 kV giving a dielectric strength of 656 V/mil.

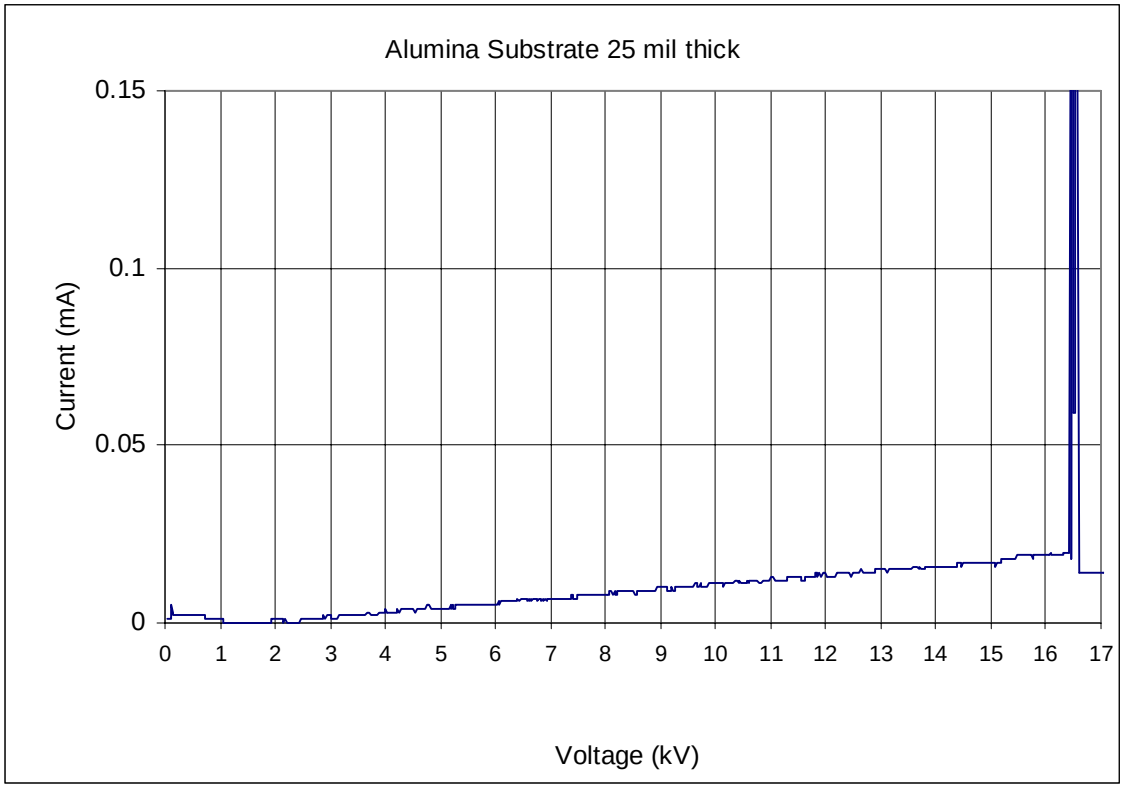

Figure 5.30. Dielectric Breakdown Voltage Results Lot 5.

5.7 Summary of Results

The data obtained from the test performed in this chapter are tabulated in appendix B. All coupons exceeded the manufacturers dielectric breakdown voltage rating. A manufactured alumina substrate tested had a dielectric strength of 656 V/mil. Moisture seemed to be present in the coupons when shipped from the manufacturer and

conditioning improved their performance when tested. The differences between conditioning 24 hours at 125 ºC or 24 hours at 200 ºC are insignificant.

Plasma spray breakdown voltage for Lot 1 ranged from a low of 4560 V for 1A (unconditioned) to a high of 7240 V for 3B (conditioned 24 hrs @ 200ºC). The breakdown voltage of coupon 1A is 242 V/mil and the breakdown voltage coupon 3B equaled 396 V/mil.

Plasma spray breakdown voltage for Lot 2 ranged from a low of 7300 V for 2A (conditioned 24 hrs @ 125ºC) to a high of 8260 V for 3B (conditioned 24 hrs @ 200ºC). The breakdown voltage of coupon 2A is 231 V/mil and the breakdown voltage coupon 3B equaled 280 V/mil. It is observed that breakdown voltage does not increase proportionally with respect to an increase in thickness.

HVOF breakdown voltage for Lot 3 ranged from a low of 5730 V for 1B (unconditioned) to a high of 6780 V for 3A (conditioned 24 hrs @ 200ºC). The breakdown voltage of coupon 1B is 764 V/mil and the breakdown voltage coupon 3A equaled 972 V/mil.

HVOF breakdown voltage for Lot 4 ranged from a low of 6420 V for 1A (unconditioned) to a high of 7780 V for 3B (conditioned 24 hrs @ 200ºC). The breakdown voltage of coupon 2A is 451 V/mil and the breakdown voltage coupon 3B equaled 562 V/mil. As with the plasma spray process, it is observed that breakdown voltage does not increase proportionally with respect to an increase in thickness. It is also observed that the HVOF process provides a higher dielectric strength per mil of thickness, which can be attributable to the HVOF process providing a denser coating.

Leakage current tests show similar results on all coupons in that unconditioned coupons contain trapped moisture and have a higher leakage current compared to conditioned coupons. All conditioned coupons exhibited less than 10 nA of leakage current at voltages less than 1400 V. It is observed that coupons from the HVOF process allow current spikes above 1400-1600 V. The spikes are not associated with trapped moisture since they occur, but not as pronounced, in the conditioned coupons.

5.8 Conclusion

The data presented in this chapter was obtained through tests conducted in the Microelectronics Laboratory of the Bradley Department of Electrical and Computer Engineering at Virginia Polytechnic Institute & State University. The SEM pictures were obtained through cooperation with the Geology Department at Virginia Polytechnic Institute & State University.

Dielectric breakdown voltage increases disproportionally to an increase in coating thickness. Coatings produced by the HVOF process have a higher dielectric strength per thickness than do coatings produced by the plasma spray process. This behavior can be attributable to HVOF coatings having a higher density.

Leakage currents are similar between the two processes up to 1400 V. At 1400 V, the HVOF process has current spikes that cannot be recorded by the direct-voltage leakage current test, due to the test apparatus' sensitivity. The leakage current spikes exceed the resolution of the test apparatus but remain well below the leakage at breakdown. No explanation is readily available for this effect. The answer might be associated with a minimal thickness required or within the microstructure of the coating. Only additional testing of these parameters can validate or dismiss these hypotheses.

CHAPTER 6

CONCLUSIONS AND FUTURE DIRECTIONS

This thesis is concerned with the topic of electronic power module packaging and the components that make up electronic power modules. The research conducted by the Microelectronics Laboratory of the Bradley Department of Electrical and Computer Engineering at Virginia Polytechnic Institute & State University shows the direct-voltage dielectric breakdown and direct-voltage leakage current of thermal sprayed plasma and HVOF alumina ceramic. All test coupons, constructed of and AlSiC MMC baseplate with thermal spray alumina ceramic applied as a dielectric isolation layer, exceeded the manufactures rating for dielectric strength. The plasma spray process produced dielectric strengths of the order 242-396 V/mil and the HVOF spray process produced dielectric strengths of the order 451-972 V/mil. A manufactured alumina substrate tested had a dielectric strength of 656 V/mil. The observations of the researcher are that the denser the alumina, the higher the dielectric strength.

The maximum operating voltage of common electronic power modules currently built is approximately 1600 V due to the limitations of IGBT transistors available. All coupons tested for leakage current had less than 10 nA of leakage current at 1600 V. This figure seems to be an acceptable level considering the amount of power to be dissipated by the electronic devices.

Environmental moisture exposure is a concern that needs to be addressed as evident from the data and measurements conducted in this research work. All coupons tested as shipped and exposed to the environment had significant lower dielectric strengths compared to coupons conditioned to remove trapped moisture. Thermal

sprayed alumina ceramic coatings will need to be conditioned and then hermetically sealed to prevent reabsorption of moisture.

The ability to use thermal spray alumina ceramic as an isolation layer in electronic devices will play an important role in reducing the production costs producing future power electronic components. Most future electronic applications seem to lie in the power electronic industry due to the desire to provide an isolation layer between a power device and a heat spreader. Production costs are lowered by the reduction of metallization layers needed while maintaining the manufacturing of reliable products. Recent developments in better spray techniques will make thermal spray alumina desirable to additional applications. With new developments in the Top Gun ™ spray process, HVOF thermal spray coatings will be used in an increasing number of electronic applications.

Appendix A

Labview™ Program HPOWER1.VI

HPOWER1.VI
08/17/98 04:29 PM

Connector Pane

HPOWER1.VI

A device connected to a GPIB bus can be written to or be read from using this
the device, choose Read or Write or both, type in the characters to be writte
both Read and Write, the VI will write to the device first, then read from the
should initialize the GPIB address according to the device's specifications w

Front Panel

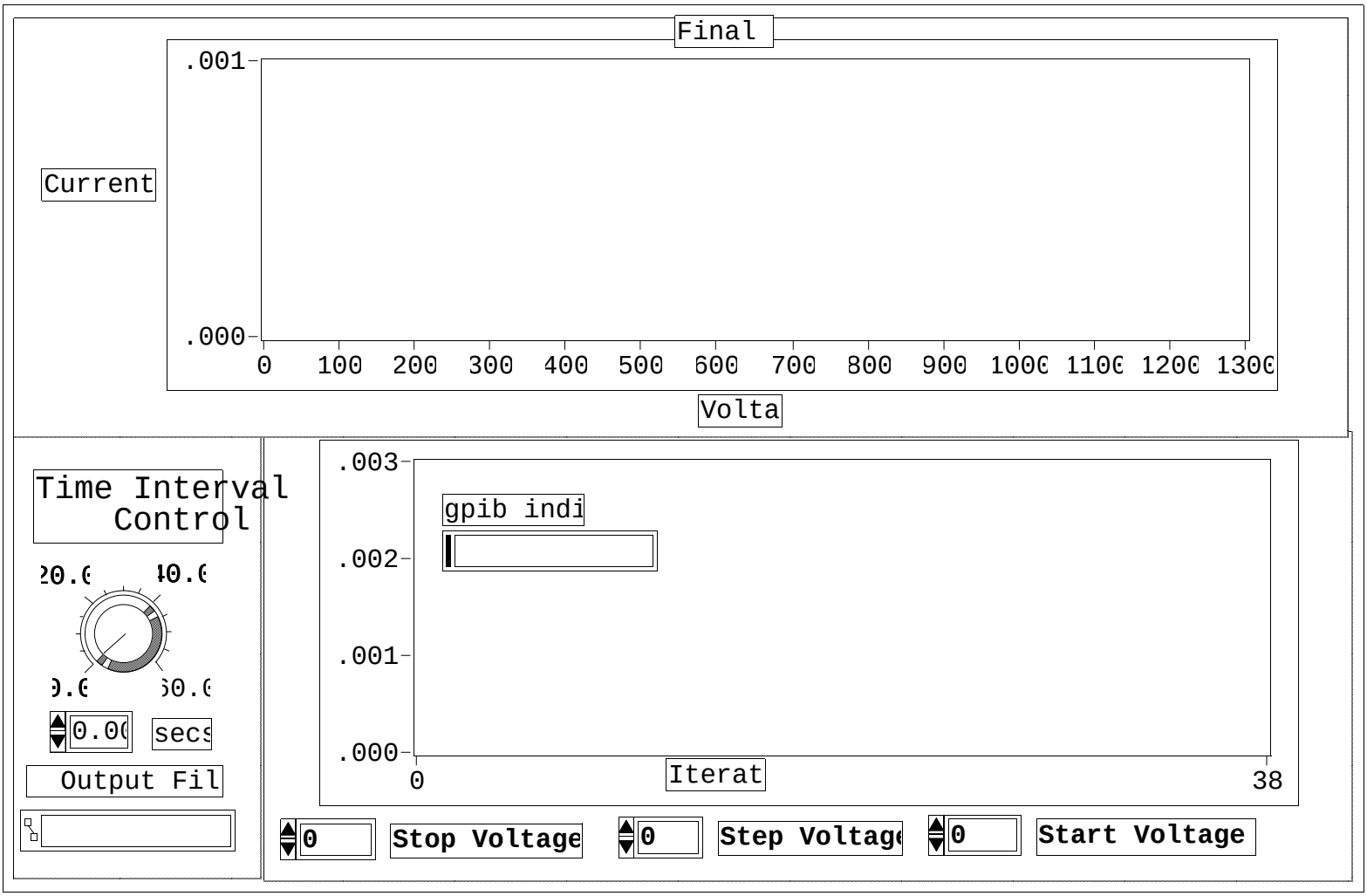

Controls and Indicators

Time Interval Control

Start Voltage

Stop Voltage

Step Voltage

HPOWER1.VI
08/17/98 04:29 PM

Write Status

Read Status

Output Characters

gpib indicator

Block Diagram

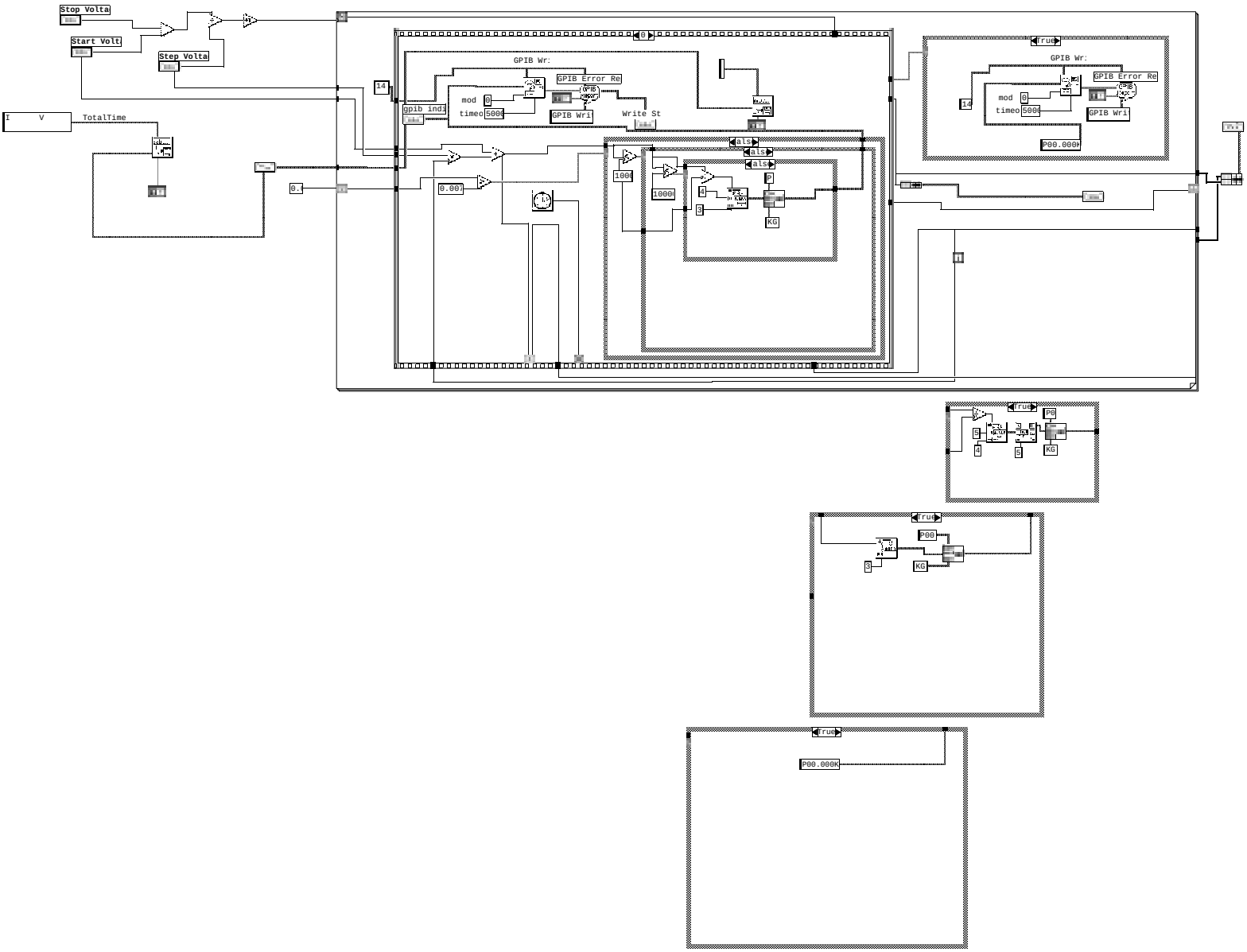

HPOWER1.VI
08/17/98 04:29 PM

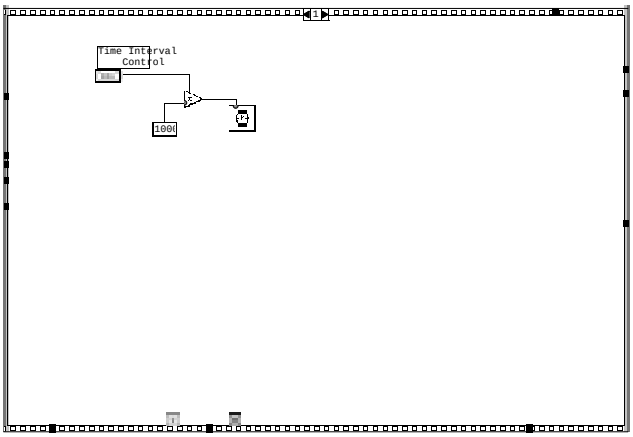

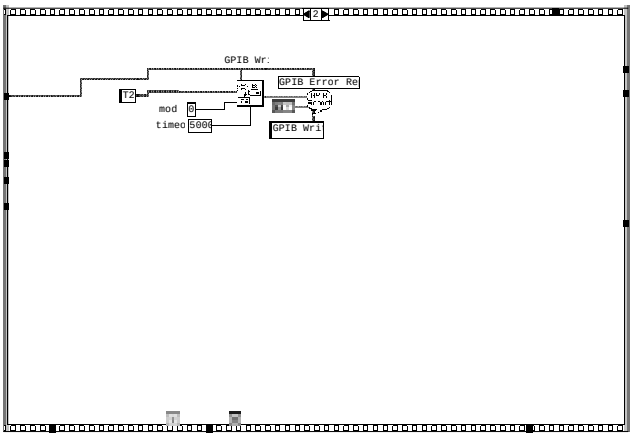

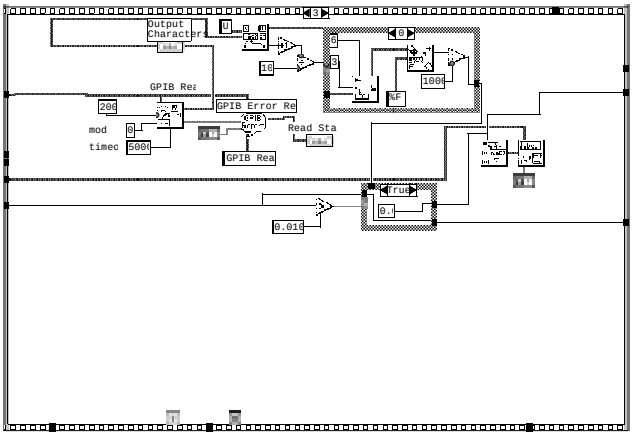

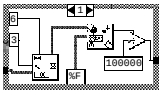

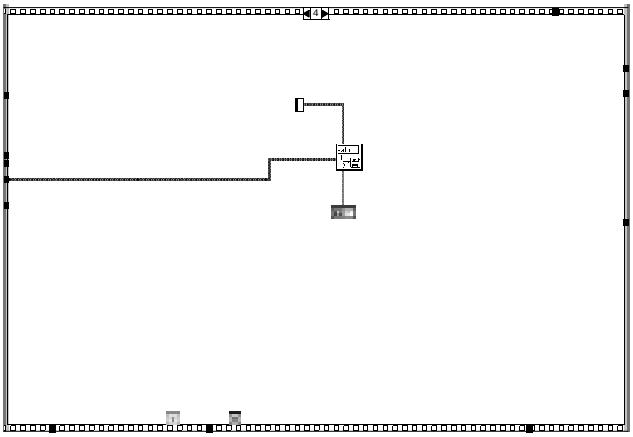

HPOWER1.VI
08/17/98 04:29 PM

HPOWER1.VI
08/17/98 04:29 PM

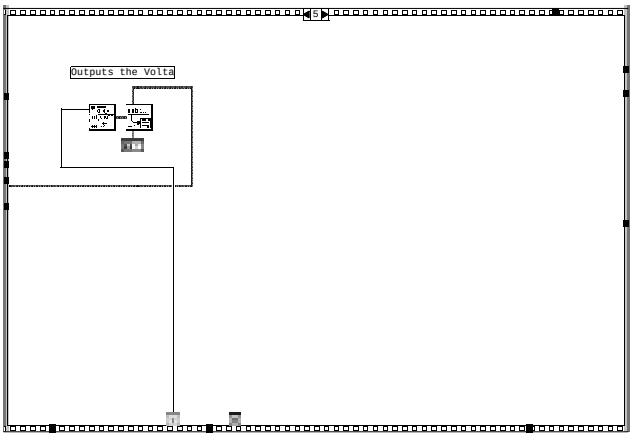

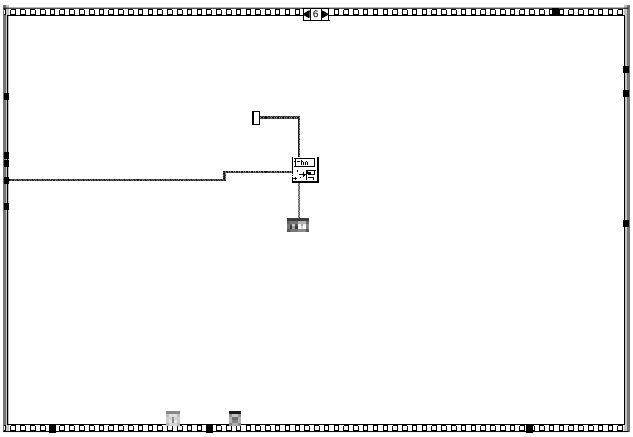

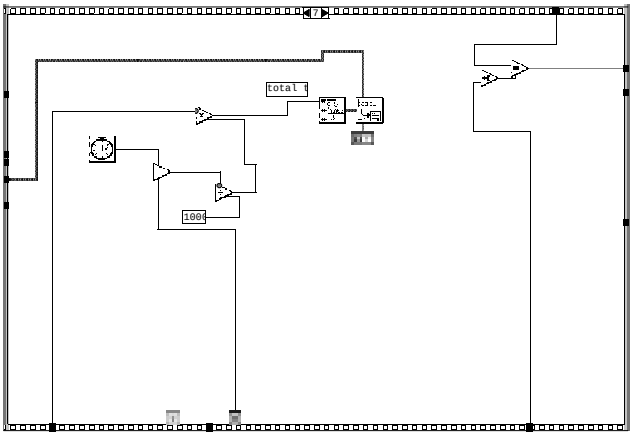

Position in Hierarchy

HPOWER1.VI
08/17/98 04:29 PM

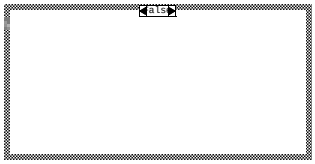

HPOWER1.VI
08/17/98 04:29 PM

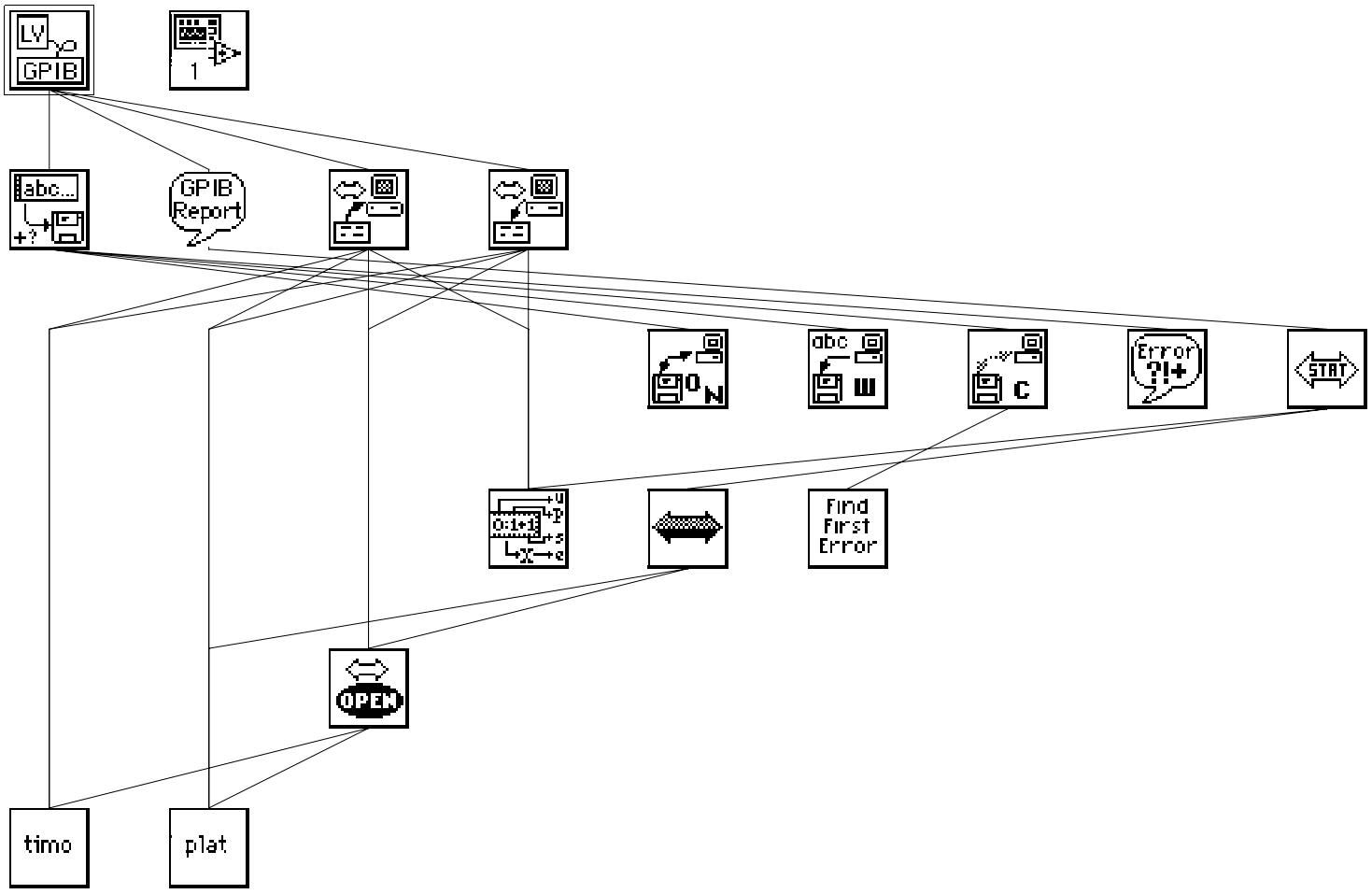

List of SubVIs

GPIB Write.vi
C:\LABVIEW\vi.lib\INSTR\GPIBTRAD.LLB\GPIB Write.vi

GPIB Read.vi
C:\LABVIEW\vi.lib\INSTR\GPIBTRAD.LLB\GPIB Read.vi

GPIB Error Report.vi
C:\LABVIEW\vi.lib\SMPLGPIB.LLB\GPIB Error Report.vi

Write Characters To File.vi
C:\LABVIEW\vi.lib\UTILITY\FILE.LLB\Write Characters To File.vi

History

"HPOWER1.VI History"
Current Revision: 123

Appendix B

Thickness Data and Breakdown Results

Substrate A

TYPE	Lot#	1st	2nd	3rd	4th	Avg. Thickness (mil)	Breakdown Voltage (V)	Breakdown Voltage (Volts/mil)
Plasma Alumina	L1-1	17.7	20.5	19.4	17.8	18.85	4560	242
Baked 24hr @ 125 C	L1-2	19.2	18.6	18.4	19.3	18.875	7010	371
24hr @ 200C	L1-3	18.2	16.4	18.2	18	17.7	5860	331
	L1-4	17.8	16.8	18.2	17.3	17.525		
	L1-5	16.3	18.7	18.9	16.3	17.55		
Plasma Alumina	L2-1	32.2	27.4	27.7	32.9	30.05	7580	252
Baked 24hr @ 125 C	L2-2	30.7	31.2	31.1	33.6	31.65	7300	231
24hr @ 200C	L2-3	32.7	27.2	29.2	30.4	29.875	7440	249
	L2-4	33.4	32	31.6	31	32		
	L2-5	32.1	29.3	31.9	30.9	31.05		
HVOF Alumina	L3-1	7.4	7.7	7.9	7.9	7.725	5920	766
Baked 24hr @ 125 C	L3-2	7.4	7.2	7	7.2	7.2	6220	864
24hr @ 200C	L3-3	6.8	7.6	6.9	6.6	6.975	6780	972
	L3-4	6.8	6.4	6.6	7.1	6.725		
	L3-5	6.6	6.6	6.4	6.4	6.5		
HVOF Alumina	L4-1	14.1	14.3	14.3	14.3	14.25	6420	451
Baked 24hr @ 125 C	L4-2	12.6	12.9	13.9	13.7	13.275	7340	553
24hr @ 200C	L4-3	13.6	13.8	14	13.5	13.725	6840	498
	L4-4	13.4	13.6	14.2	13.8	13.75		
	L4-5	14.6	14.5	15	15.4	14.875		

Substrate B

TYPE	Lot#	1st	2nd	3rd	4th	Avg. Thickness (mil)	Breakdown Voltage (V)	Breakdown Voltage (Volts/mil)
Plasma Alumina	L1-1	21.6	17.5	16.5	21.2	19.2	5780	301
Baked 24hr @ 125 C	L1-2	18	17.7	17.9	18	17.9	6650	372
24hr @ 200C	L1-3	17.3	18.5	20.1	17.2	18.275	7240	396
	L1-4	16.6	19.3	21.5	16.4	18.45		
	L1-5	16.1	18.9	19.2	16.2	17.6		
Plasma Alumina	L2-1	33.5	28	27.7	32.5	30.425	7560	248
Baked 24hr @ 125 C	L2-2	33.5	31.3	29.9	35.5	32.55	8240	253
24hr @ 200C	L2-3	29.1	30	31.2	27.8	29.525	8260	280
	L2-4	32.7	32.3	33.6	32.5	32.775		
	L2-5	30.4	33.2	35	27.9	31.625		
HVOF Alumina	L3-1	7.3	7.5	7.6	7.6	7.5	5730	764
Baked 24hr @ 125 C	L3-2	7.2	7	7.3	7.2	7.175	6530	910
24hr @ 200C	L3-3	7.5	7.5	7.8	8	7.7	5980	777
	L3-4	6.9	5.8	5.9	7	6.4		
	L3-5	6.7	6.6	6.4	7	6.675		
HVOF Alumina	L4-1	15	14.6	14.5	14.6	14.675	7020	478
Baked 24hr @ 125 C	L4-2	14.1	14.9	13.6	13.2	13.95	6540	469
24hr @ 200C	L4-3	13.4	14.1	14.5	13.4	13.85	7780	562
	L4-4	13.3	13.2	13.6	13.5	13.4		
	L4-5	14.3	14	14.9	14.9	14.525		

BIBLIOGRAPHY

1. A. Lostetter, F. Barlow, and A. Elshabini, “Thermal Evaluation and Comparison Study of Power Baseplate Materials”, Advancing Microelectronics, Vol.25, No.1, pp.25-27, Jan./Feb. 1998.

2. V. Meringolo, *Thermal Spray Coatings*, Atlanta: TAPPI Press, 1983, Chapter 1, pp.7-8.

3. R. Tucker, Jr., “Thermal Spray Coatings”, ASM Handbook, Vol. 5, pp. 497-508, 199?.

4. J. Hwang, *Modern Solder Technology for Competitive Electronics Manufacturing*, New York: McGraw-Hill, 1996, pp. 72.

5. R. Palmer, “Using a Plasma Sprayed Alumina Coating as an Electrical Insulator with Semiconductor Device Packages”, Thermal Spray: International Advances in Coatings Technology Conference Proceedings, Materials Park: ASM International, 1992, pp. 825-828.

6. R. Suryanarayanan, *Plasma Spraying*, Singapore: World Scientific Publishing Co. Pte. Ltd., 1993, 103-114.

7. A. Kobayashi, “Property of an Alumina Coating Sprayed with a Gas Tunnel Plasma Spraying”, Thermal Spray: International Advances in Coatings Technology Conference Proceedings, Materials Park: ASM International, 1992, pp. 57-61.

8. D. Matejka and B. Benko, *Plasma Spraying of Metallic and Ceramic Materials*, New York: John Wiley & Son, 1989, pp.11-48.

9. E. Pfender, “Fundamental Studies Associated with the Plasma Spray Process”, Thermal Spray: Advances in Coatings Technology Conference Proceedings, Materials Park: ASM International, 1988, pp. 1-9.

10. R. Smart and J. Catherall, *Plasma Spraying*, London: Mills & Boon Limited, 1972, Chapter 4, pp. 42-47.

11. H. Kreye and U. Granz-Schnibbe, “High Velocity Flame Spraying of Chromium Oxide and Aluminum Oxide”, Thermal Spray Research and Applications Conference Proceedings, Materials Park: ASM International, 1990, pp. 575-577.

12. R. Thorpe and M. Thorpe, “High Pressure HVOF-An Update”, Conference Proceedings Thermal Spray Coatings: Research, Design and Applications, Materials Park: ASM International, 1993, pp. 199-203.

13. T. Peterman, “The High Volume Production of Plasma Prayed Dielectric Coatings”, Thermal Spray: International Advances in Coatings Technology Conference Proceedings, Materials Park: ASM International, 1992, pp. 309-320.

14. R. Kawase, H. Haraguchi, and T. Hamamoto, “Non-Destructive Evaluation Method for Thermal Sprayed Ceramic Coatings Using Ultrasonic Waves”, Conference Proceedings Thermal Spray Coatings: Properties, Processes and Applications, Materials Park: ASM International, 1991, pp. 187-191.

15. D. Neamen, *Semiconductor Physics & Devices 2nd Edition*, Chicago: McGraw-Hill, 1997, pp. 63-64.

16. S. Whitehead, *Dielectric Breakdown of Solids*, Oxford: University Press, 1953, pp. 23-37.

17. “Standard Test Method for Dielectric Breakdown Voltage and Dielectric Strength of Solid Electrical Insulating Materials Under Direct-Voltage Stress, D 3775-86 (Reapproved 1995)”, Annual Book of ASTM Standards, West Conshohocken: ASTM, 1996, vol. 10.01, pp. 309-313.

18. “Standard Terminology Relating to Electrical Insulation, D 1711-95”, Annual Book of ASTM Standards, West Conshohocken: ASTM, 1996, vol. 10.01, pp. 432-440.

19. “Standard Test Method for Dielectric Breakdown Voltage and Dielectric Strength of Solid Electrical Insulating Materials at Commercial Power Frequencies, D 149-95a”, Annual Book of ASTM Standards, West Conshohocken: ASTM, 1996, vol. 10.01, pp. 14-25.

20. “Standard Practice for Conditioning Plastics and Electrical Insulating Materials for Testing, D 618-95”, Annual Book of ASTM Standards, West Conshohocken: ASTM, 1996, vol. 08.01, pp. 36-38.

21. L. Wells, *Labview™, Student Edition User’s Guide*, New Jersey: Prentice Hall,1995.

22. “Standard Test Methods for Thickness of Solid Electrical Insulation, D 374-94”, Annual Book of ASTM Standards, West Conshohocken: ASTM, 1996, vol. 10.01, pp. 166-187.

Vita

Charles W. Mossor was born in Richwood, West Virginia on July 3rd, 1963. Charles grew up in Monroe County, West Virginia, where he loved to explore how things worked and fix things that were broken.

In 1982, Charles married his childhood sweetheart and pursued a career in farming. After the blizzard of 1993, a career change was needed and Charles decided to pursue an Electrical Engineering degree. Charles graduated Bluefield State College as the 1997 Valedictorian with a B.S. Degree in Electrical Engineering Technology and started at Virginia Polytechnic Institute and State University in The Bradley Department of Electrical and Computer Engineering that Fall Semester in pursuit of a Masters Degree in Electrical Engineering.

The next several years will be interesting as he will pursue a career in the Electrical Engineering field while working also on an MBA Degree. Upon completion of an MBA Degree, Charles plans to become a Technical Manager.